

Level statistics across the many-body localization transition

Piotr Sierant¹ and Jakub Zakrzewski^{1,2,*}

¹*Instytut Fizyki imienia Mariana Smoluchowskiego, Uniwersytet Jagielloński, ulica Profesora Stanisława Łojasiewicza 11, PL-30-348 Kraków, Poland*

²*Mark Kac Complex Systems Research Center, Uniwersytet Jagielloński, ulica Profesora Stanisława Łojasiewicza 11, PL-30-348 Kraków, Poland*



(Received 14 August 2018; revised manuscript received 2 March 2019; published 22 March 2019)

Level statistics of systems that undergo many-body localization transition are studied. An analysis of the gap ratio statistics from the perspective of inter- and intrasample randomness allows us to pin point differences between transitions in random and quasirandom disorder, showing the effects due to Griffiths rare events for the former case. It is argued that the transition in the case of random disorder exhibits universal features that are identified by constructing an appropriate model of intermediate spectral statistics which is a generalization of the family of short-range plasma models. The considered weighted short-range plasma model yields a very good agreement both for level spacing distribution including its exponential tail and the number variance up to tens of level spacings outperforming previously proposed models. In particular, our model grasps the critical level statistics which arise at disorder strength for which the intersample fluctuations are the strongest. Going beyond the paradigmatic examples of many-body localization in spin systems, we show that the considered model also grasps the level statistics of disordered Bose- and Fermi-Hubbard models. The remaining deviations for long-range spectral correlations are discussed and attributed mainly to the intricacies of level unfolding.

DOI: [10.1103/PhysRevB.99.104205](https://doi.org/10.1103/PhysRevB.99.104205)

I. INTRODUCTION

It is 90 years already since Wishart in a seminal paper [1] introduced the concept of random matrices into science. His original aim was to generalize the chi-squared distribution to multiple dimensions, random symmetric non negative matrices played then the role of random variables. The corresponding Wishart distribution found many applications from modern random matrix theory [2] to various applications in physics [3–6], wireless communications [7] financial data for large portfolios [8] etc.

The next big step came with the introduction of Gaussian ensembles and the realization of Wigner and others [9] that spectra for usually unknown complex nuclear Hamiltonians may be understood statistically using properties of these ensembles obeying appropriate symmetries. It became a textbook knowledge that there exist exactly three universality classes [10,11]: the Gaussian orthogonal ensemble (GOE) corresponds to systems invariant with respect to (generalized) time reversal, the Gaussian unitary ensemble corresponds to systems with broken time-reversal invariance, and the symplectic ensemble corresponds to half-integer spin systems with preserved time-reversal invariance and no other symmetries present. Thus, since the sixties, it was the common knowledge that spectra of many-body interacting systems are statistically well described by random matrix theory (RMT). Further justifications of successes of RMT come from the theory of Dyson yielding the Gaussian ensembles from an appropriate statistical mechanics description [12–15].

An interesting development appeared in the eighties—the conjecture that statistical properties of spectra of systems chaotic in the classical limit are faithful to random matrix predictions [16]. This came as a surprise—even simple single-particle Hamiltonians containing no randomness and represented by large, very sparse (due to strong selection rules in appropriately chosen basis) matrices were statistically faithful to RMT predictions as revealed, e.g., in the study of hydrogen atom spectrum in the presence of strong magnetic field inducing the so called quadratic Zeeman coupling [17]. More precisely, after unfolding the levels (obtaining the mean density of states equal to unity), the remaining fluctuations were faithfully represented by predictions of RMT [18] as shown by nearest-neighbor spacing distribution- $P(s)$, the so called number variance (i.e., the variance of the number of levels in an interval of length L), correlation functions, etc. The same measures indicated, however, that the transition from the chaotic to integrable situation (described by Poisson ensemble of uncorrelated levels for systems of large dimensions [18]) seems system specific and determined by the structure of the underlying classical mechanics in the mixed phase space [19].

Similar transition from extended to localized states, as revealed, e.g., by a change of level statistics from GOE-like to Poisson-like, appears in the Anderson localization transition. The corresponding level statistics has been addressed in the seminal paper [20] followed by other important developments [21–23] to mention early contributions—for a review see Ref. [24]. In those cases, a single-particle problem in disordered medium was addressed.

Recent years provided another important example of such a transition between ergodic (describable by standard Gaussian RMT) and integrable limits—the many-body

*jakub.zakrzewski@uj.edu.pl

localization (MBL). While for weak disorder many-body interacting systems behave as expected for a long time being ergodic and following Gaussian RMT predictions, for a sufficiently strong disorder a gradual (for finite systems sizes) crossover to localized situation occurs [25]. This phenomenon attracted an enormous interest in the last 10 years as it provides a robust example of nonergodic behavior in a complex many-body system. Instead of effectively thermalizing (as suggested by the eigenvector thermalization hypothesis (ETH) [26]), such strongly disordered systems often remember their initial state as manifested in a series of spectacular experiments [27–29]. Already early theoretical studies [30] showed that a transition to MBL situation is accompanied by a change of level statistics from that corresponding to GOE to Poisson-like for MBL.

Importantly, it has been suggested that MBL phase is indeed integrable [31,32], namely, in MBL phase, a complete set of local integrals of motions (LIOMs) may be defined. On one side, finding LIOMs provides information about the system for a given disorder realization (LIOMs are disorder realization dependent), on the other side, the very existence of LIOMs explains the Poissonian statistics observed deep in the localized phase. While the two extremal situations—the metallic, GOE-like ergodic behavior for a weak disorder and the full MBL phase—seem to be presently quite well understood, it is desirable to understand and describe the nature of the ergodic-MBL transition.

The problem is not simple; it has been found, in particular, that the nature of the disorder plays a decisive role in the character of the transition [33,34]. Intrasample randomness was identified as the dominant feature for quasiperiodic disorder (QPD) while the intersample randomness is an essential property of transition for purely random disorder (RD). Those important observations were made studying the entanglement entropy behavior.

In this work, we show that a proper analysis of gap ratio statistics allows us to get similar insight on the randomness of system in MBL transitions as the entanglement entropy [33]. Our method is conceptually simpler as it relies only on the spectrum of the system and as such can be straightforwardly used in studies of various complex systems. Secondly, this analysis, as a byproduct, gives hints on the construction of universal model of level statistics for MBL transition which we provide generalizing earlier attempts [20,35,36]. We introduce a weighted short-range plasma model (wSRPM) and argue that it describes faithfully the level statistics during the whole crossover between ergodic and MBL phases at system sizes accessible in exact diagonalization studies. Taking into account the intersample randomness (an inherent feature of MBL transition in systems with random disorder), the proposed model grasps correctly not only the bulk properties of the level spacing distribution $P(s)$ but also its exponential tails and correctly reproduces the number variance, $\Sigma^2(L)$, at L of the order of tens level spacings. This implies that wSRPM reflects faithfully both short-range and long-range spectral correlations in systems across the ergodic-MBL crossover. Remaining small discrepancies are discussed in details providing a further insight into the long-range spectral correlations of the system. Furthermore, we show that the wSRPM is universal as it works across the whole ergodic to MBL crossover not only

in spin models but also in disordered bosonic and fermionic systems. We compare our results with earlier propositions [35–39] showing that the model proposed by us represents the data much more faithfully. We also discuss an alternative model of level statistics—weighted power-law random banded matrix model, which also accurately grasps spectral correlations across the ergodic-MBL crossover.

II. GAP RATIO ANALYSIS

A dimensionless ratio of consecutive energy levels gaps (referred as the gap ratio) was introduced in Ref. [30]. It is defined as $r_n = \min\{\delta_n, \delta_{n-1}\} / \max\{\delta_n, \delta_{n-1}\}$, where $\delta_n = E_{n+1} - E_n$ is an energy difference between two consecutive levels. The average gap ratio \bar{r} is different for systems with extended eigenstates (in the following we shall concentrate on the Gaussian orthogonal ensemble (GOE) for time-reversal invariant systems): $\bar{r}_{\text{GOE}} \approx 0.53$ and for localized systems $\bar{r}_{\text{Poi}} \approx 0.39$ as was analytically demonstrated in Ref. [40]. That property was used by many authors in attempts to localize the MBL transition [30,41–49].

The usual way of calculating the mean gap ratio \bar{r} is to average the r_n variable over a certain number of energy levels getting a mean gap ratio for one sample $r_S = \langle r_n \rangle_S$. Then, the mean gap ratio is obtained by averaging of r_S over disorder realizations $\bar{r} = \langle r_S \rangle_{\text{dis}}$. While, as mentioned above \bar{r} obtained in this way reflects the character of eigenstates of the system [30,41–45,47] a part of information encoded in the r_n variables is necessarily lost. Let us examine $P(r_S)$ —the distribution of the sample averaged gap ratio r_S —it provides a direct information about variations of the r_S for different disorder realizations. As an example, we consider the XXZ spin-1/2 chain with additional next-nearest-neighbor coupling (similar to that of Ref. [33])

$$H = J \sum_{i=1}^K \vec{S}_i \cdot \vec{S}_{i+1} + W \sum_{i=1}^K \cos(2\pi\zeta i + \phi) S_i^z + J_1 \sum_{i=1}^K S_i^z S_{i+2}^z, \quad (1)$$

where \vec{S}_i are spin-1/2 matrices, $\zeta = (\sqrt{5} - 1)/2$ (the golden ratio), and ϕ is a fixed phase for a given disorder realization (leading to QPD) or is random on each lattice site (leading to RD with the same on-site distribution, as in the QPD case) [33]. We fix $J = 1$ as the energy unit and we study the case of $J_1 = J$ first. Periodic boundary conditions are assumed so that $\vec{S}_{K+1} = \vec{S}_1$. For the system size $K = 16$, we consider sequences of $N = 400$ consecutive eigenvalues from the middle of the spectrum yielding a collection of r_S values for $n_{\text{dis}} = 2000$ disorder realizations. The resulting distributions $P(r_S)$ for different disorder strengths W are shown in Fig. 1.

Had all r_n been independent of each other the distribution of $r_S = \sum_{n=1}^N r_n / N$ should be Gaussian with width determined by the variance of the r_n distribution and proportional to $1/\sqrt{N}$. Despite the correlations—particularly strong for GOE—the $P(r_S)$ are Gaussian in the limiting cases of GOE and Poisson statistics. Surprisingly, the $P(r_S)$ distributions remain Gaussian for QPD across the transition.

In a striking contrast, the distributions in the RD case become strongly asymmetric with enlarged variance in the

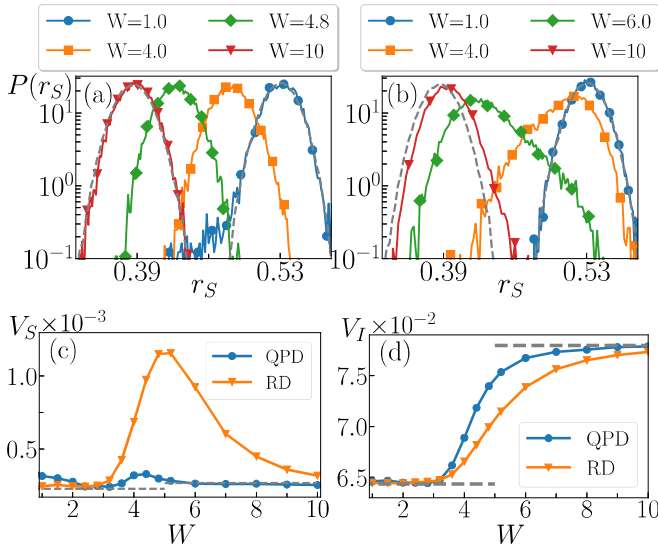


FIG. 1. (a) Distributions $P(r_S)$ for quasiperiodic disorder (QPD) of strength W . Dashed lines give limiting GOE and Poisson behaviors. The tail of the $W = 1$ distribution indicates that QPD reproduces GOE statistics only approximately. (b) Distributions $P(r_S)$ for random disorder (RD). (c) The intersample variance V_S for RD and QPD and (d) the intrasample variance V_I for QPD and RD during the transition.

transition region. This reflects the intersample randomness importance for the RD and is a clear, nice manifestation of the existence of rare Griffiths regions [50–53]: for samples with \bar{r} close to GOE there exist realizations of disorder leading to r_S close to Poisson limit. Similarly, on a localized side for \bar{r} close to integrable limit there are rare events with r_S values close to GOE value. The stark difference in the $P(r_S)$ distributions between the RD and QPD cases can be quantified by calculating a variance: $V_S = \langle r_S^2 - \bar{r}^2 \rangle_{\text{dis}}$. As Fig. 1(c) shows, the intersample variance V_S has a clear peak in the MBL transition for the RD whereas it varies only slightly for the QPD.

Consider now the variance v_I of the r_S variable, $v_I = \langle r_n^2 - r_S^2 \rangle_S$. Averaged over disorder realizations $V_I = \langle v_I \rangle_{\text{dis}}$, it provides information about fluctuations of r_n within a single spectrum of the system at a certain disorder strength—characterizing intrasample randomness. As could be expected from the long-range correlations of GOE, it is small for GOE and conversely, it is maximal for Poissonian spectrum. Figure 1(d) shows that it behaves similarly for QPD and RD interpolating between the values for GOE and Poisson statistics. The transition is sharper for the system with QPD, implying that it is less affected by finite size effects [33].

Seeing that the distribution $P(r_S)$ and the variances V_S and V_I provide a valuable information about the randomness at the MBL transition, let us switch our attention to the more standard Heisenberg chain case taking $J_1 = 0$ in Eq. (1) and assuming random uniform disorder so that $W \cos(2\pi\zeta i + \phi)$ is exchanged by $h_i \in [-W, W]$ in Eq. (1), explicitly

$$H = J \sum_{i=1}^K \vec{S}_i \cdot \vec{S}_{i+1} + \sum_{i=1}^K h_i S_i^z. \quad (2)$$

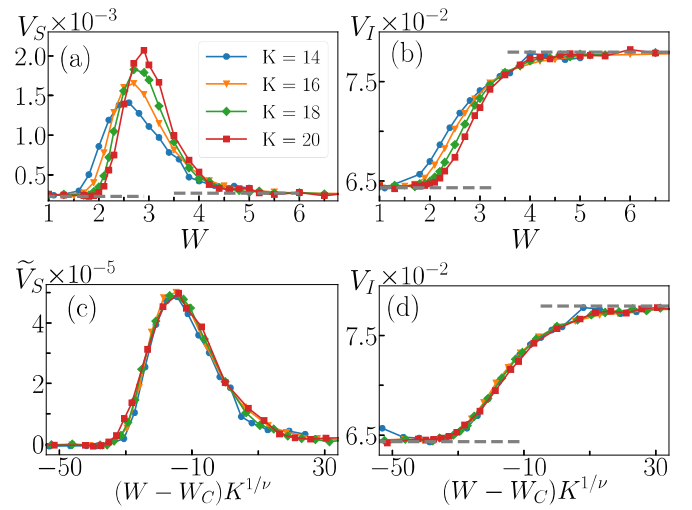


FIG. 2. (a) The variance V_S of the r_S distribution characterizing the intersample randomness, (b) the variance V_I reflecting the intrasample fluctuations in the spectrum of the system. (c) The rescaled intersample variance \tilde{V}_S and (d) the intrasample variance V_I collapse after the rescaling of the disorder strength with $W_C = 3.5$ and $\nu = 0.95$. The data are for system sizes $K \in \{14, 16, 18, 20\}$.

Despite the fact that the distribution of disorder is different and the studied model contains now nearest neighbor couplings only, the $P(r_S)$ behaves quite similarly to the case shown in Fig. 1(b) revealing strong asymmetry and broadening across the transition—as shown in Fig. 2. Particularly, the broader distributions in the transition regime suggest that one may use the maximal variance V_S as an indicator of the transition point.

A standard finite size scaling of different quantities can be performed assuming $W \rightarrow (W - W_C)K^{1/\nu}$. For \bar{r} such an analysis has been performed already [43,54] with the data collapsing to a single curve. Similar scaling may be used for the variance V_S . Observe that both the position of the maximum as well as its value depend on the system size [Fig. 2(a)].

If, together with the rescaling of the disorder strength, the variance V_S is rescaled according to $V_S \rightarrow \tilde{V}_S = (V_S - V_{\text{GOE}})/K^\kappa$ (where V_{GOE} is the intersample variance for GOE) the data for various system sizes collapse onto a single curve [Fig. 2(c)] for the exponents $\nu = 0.95(10)$, $\kappa = 1.2(1)$, and the critical disorder strength $W_C = 3.5(1)$. The scaling of the V_S will necessarily cease to work for larger system sizes as the support of the $P(r_S)$ distribution is limited by \bar{r}_{Poi} and \bar{r}_{GOE} . On the other hand, the critical disorder strength $W_C = 3.5(1)$ and the exponent $\nu = 0.95(10)$ are in nice agreement with results of [43]. A similar finite size scaling may be performed for the intrasample variance V_I with the same W_C and ν [Fig. 2(d)]. It is notable that all three measures \bar{r} , V_S and V_I scale in a very similar manner. Being interconnected they still provide different insights into physics of the system during the MBL transition.

The gap ratio analysis demonstrates that more than just an overall information about the crossover between ergodic and MBL regimes can be obtained from the r_n variables.

The considered inter- and intrasample variances V_S and V_I reflect nicely the differences between RD and QPD universality classes. Furthermore, the $P(r_S)$ distribution quantifies the intersample fluctuations of a system undergoing MBL transition and gives a particularly clear demonstration of the Griffiths regime.

Moreover, the gap ratio analysis hints how to formulate the wSRPM model of spectral statistics across the MBL transition for the random disorder—namely, the ensemble we are looking for should take into account the large intersample randomness of the RD case. The problem of construction of such an ensemble will be considered in the remaining part of the manuscript. We start by reviewing the existing models of level statistics in the MBL transition.

III. LEVEL STATISTICS IN MBL TRANSITION

A number of models for intermediate statistics in the MBL transition have been proposed in Refs. [35,36,38,39]. In this section, we compare level spacing distributions $P(s)$ and number variances $\Sigma^2(L)$ predicted by those models with data for the standard model of MBL—XXZ spin-1/2 chain Eq. (2), studied already in the previous section. As we have seen this model undergoes a transition to MBL at $W_C \approx 3.5$ in the thermodynamic limit $K \rightarrow \infty$, in the center of the spectrum ($W_C \approx 3.7$ was obtained in Ref. [43]). Figure 3 shows level spacing distribution $P(s)$ and number variance $\Sigma^2(L)$ for the system (2) of size $K = 16$ at disorder strength $W = 1.9$ compared with predictions of different proposed models [35,38,39] of the flow of level statistics between GOE and PS limits supplemented by data for the short-range plasma model (SRPM) [55]. The numerical data for spacing distribution and the number variance for XXZ spin chain are fitted with those models.

Mean-field plasma model. The work [35] describes the flow of level statistics across the MBL transition. Close to the ergodic regime a mean-field plasma model [21] with an effective power-law interaction between energy levels is proposed. It predicts the level spacing distribution and the number variance to be

$$P(s) = C_1 s^\beta e^{-C_2 s^{2-\gamma}} \quad \text{and} \quad \Sigma_2(L) \propto L^\gamma \quad (3)$$

with $C_{1,2}$ determined by normalization conditions $\langle 1 \rangle = \langle s \rangle = 1$. The exponents β and γ reflect a local repulsion of energy levels and an effective range of interactions between energy levels. They are treated as fitting parameters which vary across the transition. Note that for $\gamma = 1$ the eigenvalues are interacting only locally leading to semi-Poisson statistics

$$P(s) \propto s^\beta e^{-(\beta+1)s} \quad \text{and} \quad \Sigma_2(L) \propto \frac{1}{\beta+1} L. \quad (4)$$

Between GOE and Poisson limits the exponent γ satisfies $0 < \gamma < 1$. It follows from (3) that tail of the level spacing distribution decays faster than exponentially with s and that the number variance $\Sigma^2(L)$ increases as a power law of L . The level spacing distribution and the number variance predicted by this model are denoted by the solid violet line in Fig. 3: the values of β and γ are obtained by the least square fit to the bulk of $P(s)$ and the multiplicative factor in front of the $\Sigma^2(L)$ is treated as the third fitting parameter. While the bulk

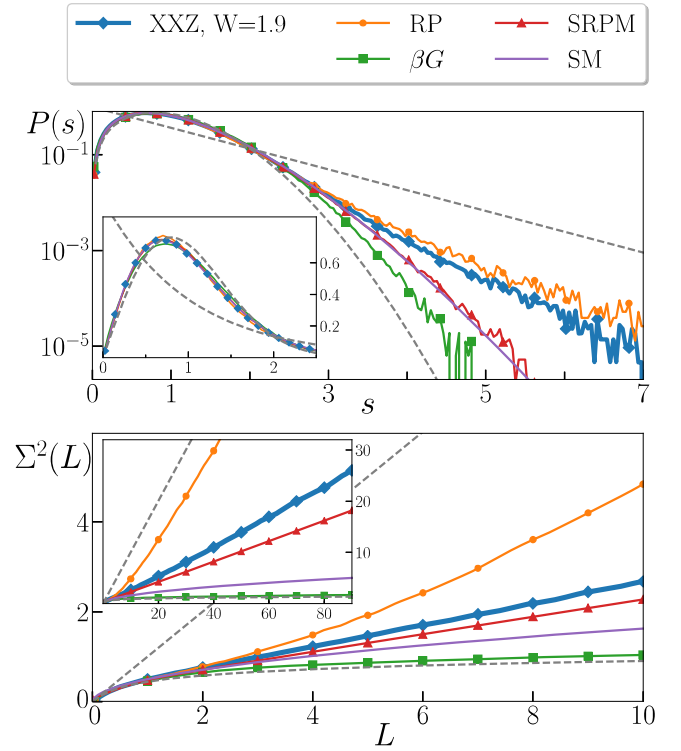


FIG. 3. (Top) Level spacing distribution $P(s)$ for XXZ spin chain (2) of size $K = 16$ at disorder strength $W = 1.9$ compared with predictions of various models of the flow of level statistics between GOE and PS limits in the MBL crossover discussed in the main text. The vertical axis of the main plot is logarithmic to enable the comparison of tails of the distributions, inset shows the data in doubly linear scale; RP: the Rosenzweig-Porter model at $\sigma = 0.0016$; βG : β Gaussian ensemble with $\beta = 0.81$; SRPM: short-range plasma model with the range of interactions $h = 5$; SM: the mean-field model (3). (Bottom) The number variance $\Sigma^2(L)$ for the same system, inset shows the long-range behavior of $\Sigma^2(L)$ which encodes long-range spectral correlations of eigenvalues. Gray dashed lines correspond to level spacing distributions and number variances for GOE and PS limits.

of the level spacing distribution is nicely recovered, the tail of the $P(s)$ distribution and the number variance are clearly not matching the data for $W = 1.9$.

This two features were shown to be not obeyed by a system across the MBL crossover in [36] where it was demonstrated that the level spacing distributions decay exponentially with s . At the same time the number variance increases as L^γ with $\gamma > 1$ close to the ergodic phase and as the system becomes more localized it becomes asymptotically linear for large L .

Rosenzweig-Porter ensemble. Another work [38] suggest that Rosenzweig-Porter (RP) ensemble can be appropriate to describe the MBL transition. Multifractal properties of eigenvectors of this model, which is defined as an ensemble of real symmetric (for $\beta = 1$ orthogonal class relevant for us) random matrices $M = (M_{ij})$ of size $n \times n$ with matrix elements being independent Gaussian variables with zero average values $M_{ij} = 0$ and

$$\langle M_{ii}^2 \rangle = 1, \quad \text{and} \quad \langle M_{ij}^2 \rangle = \sigma/2 \quad (5)$$

were studied in Ref. [56]. The dotted line in Fig. 3 shows the obtained level spacing distribution and the number variance which fits best the data for the XXZ spin chain at $W = 1.9$. The presented data are for $n = 3000$ and $\sigma = 0.0016$ and are in rather poor agreement even regarding the bulk of the $P(s)$ distributions. Moreover, at $L \gtrsim 3$, the number variance bends abruptly upwards—a feature which we do not observe for the $W = 1.9$ data. Similar trend persists at larger disorder strengths W indicating that one cannot reproduce both the level spacing distribution and the number variance $\Sigma^2(L)$ of the XXZ spin chain across the MBL crossover within the RP ensemble.

β -Gaussian ensemble. The two remaining models [39,55] can be specified by a joint probability distribution function (JPDF) of eigenvalues. A JPDF for a random matrix ensemble can be written as the probability distribution of a one-dimensional gas of classical particles with total energy $W(E_1, \dots, E_n)$

$$\mathcal{P}(E_1, \dots, E_N) = Z_N^{-1} \exp(-\beta W(E_1, \dots, E_n)), \quad (6)$$

where Z_N is a normalization constant and the total energy

$$W(E_1, \dots, E_n) = \sum_i U(E_i) + \sum_{i < j} V(|E_i - E_j|) \quad (7)$$

is determined by the trapping potential $U(E)$ and interparticle interactions $V(|E - E'|)$. For instance, for harmonic trapping potential $U(E) \propto E^2$, and logarithmic interactions $V(|E - E'|) = -\ln(|E - E'|)$ and $\beta = 1$ one recovers from (6) the JPDFs for GOE, for which the interactions in (6) are between all pairs of eigenvalues which reflects the long-range spectral correlations of the GOE ensemble.

One way of constructing an ensemble with statistical properties intermediate between GOE and PS is to put a rational $\beta \in [0, 1]$ into JPDF (6)—in such a way a β -Gaussian ensemble (β GE) arises. A recent work [39] uses β GE to describe the level spacing distribution $P(s)$ and the gap ratio distribution in the MBL transition. Setting up appropriate tridiagonal matrices [57] of size $n = 10^5$ and diagonalizing them, we obtain $P(s)$ and $\Sigma^2(L)$ for this ensemble—denoted by the green line with squares in Fig. 3. The agreement of this model with XXZ numerical data in the bulk of the $P(s)$ is not perfect. The disagreement in the tail of the $P(s)$ and the number variance is even more pronounced. Long-range correlations of eigenvalues in β GE are visible in the spectral rigidity of the spectrum—for the acquired data the number variance grows only logarithmically, just like in the GOE case, in a violent disagreement with the XXZ data. Thus, contrary to statements in Ref. [39] based on short-range correlations only, the β GE is not a good candidate to describe the flow of level statistics between GOE and PS regimes across the MBL transition.

Short-range plasma models. Another way of constructing intermediate level statistics is to restrict the range of the logarithmic interactions in (6) to a finite number h , which leads to a family of short-range plasma models (SRPMs) [55]. Consider $N \rightarrow \infty$ particles in a ring geometry $E_0 < E_1 < \dots < E_N < E_{N+1}$, $E_{N+1+k} = E_k \bmod N$ with logarithmic interaction among h neighboring eigenvalues so that the

JPDF is given by

$$\mathcal{P}_h^\beta(E_1, \dots, E_N) = Z_N^{-1} \prod_{i=0}^N |E_i - E_{i+1}|^\beta \dots |E_i - E_{i+h}|^\beta. \quad (8)$$

For integer values of h and β , this model can be analytically solved yielding the level spacing distribution

$$P_h^\beta(s) = s^\beta W(s) e^{-(h\beta+1)s}, \quad (9)$$

where $W(s)$ is a polynomial. The corresponding number variance has asymptotically linear behavior:

$$\Sigma_{h,\beta}^2(L) \xrightarrow{L \rightarrow \infty} \frac{L}{h\beta + 1}. \quad (10)$$

The SRPM can be solved analytically—see Appendix A for details. While grasping the bulk of the level spacing distribution $P(s)$ accurately, the SRPM model does not outperform the mean-field model [Eqs. (3) and (4)]. One still does not obtain the correct tails of the level spacing distribution $P(s)$ or the correct slope of the number variance $\Sigma^2(L)$ —see the line with triangles in Fig. 3.

IV. THE WEIGHTED SRPM MODEL

The preceding section shows that the analyzed models reproduce the bulk of the level spacing distribution and hence grasp purely local correlations of eigenvalues of a system in ergodic to MBL crossover. However, when tails of the level spacing distributions as well as the number variance are considered, the differences between data for XXZ spin chain and the predictions of the models are apparent. This shows that the models do not faithfully reproduce correlations between eigenvalues on scales larger than few level spacings. The mean-field plasma model, β -Gaussian ensemble and SRPMs tend to underestimate the number variance predicting stronger long-range correlations between eigenvalues than are actually observed across the MBL crossover. The opposite is true for the RP ensemble. All in all, the SRPM with its asymptotically exponentially decaying level spacing distribution and asymptotically linear number variance gives predictions closest to the data for XXZ spin chain. For that reason, we choose the SRPM as a basic building block of a more complicated, *weighted* ensemble which, by construction, takes into account another feature of the MBL crossover—the large intersample randomness.

Results of Sec. II indicate that large intersample randomness is an inherent feature of the MBL transition in systems with purely random disorder. It manifests itself in shape of a distribution $P(r_S)$ of the gap ratio for a single disorder realization $r_S = \langle r_n \rangle_S$, which significantly broadens in the regime of MBL transition. The broadening of $P(r_S)$ shows that system which has predominantly ergodic features becomes more localized for certain disorder realizations—the converse statement for mostly localized system is also true. The small fraction of events for which the system is more localized than usually reveals itself in the tail of the level spacing distribution and in the number variance. For instance, consider an ensemble of matrices created in such a way that with probability $1 - p$ the matrix is taken from GOE and with probability

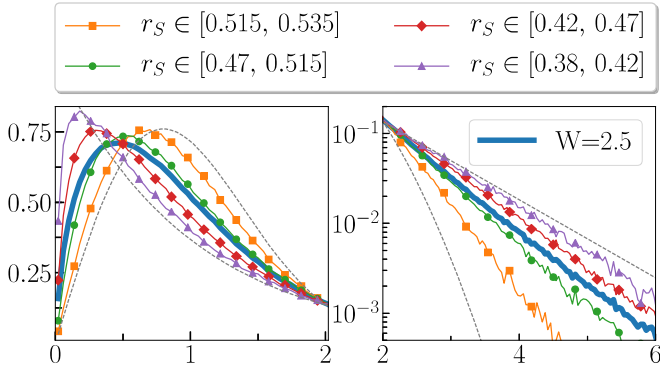


FIG. 4. Level spacing distribution $P(s)$ for XXZ spin chain (2) of size $K = 16$ at disorder strength $W = 2.5$ (solid blue line): (left) lin-lin and (right) lin-log scales to facilitate comparison of tails of $P(s)$. Selecting disorder realizations for which r_S is from a given interval results in statistics with properties which vary between those of an ergodic and nearly localized system. The gray dashed lines correspond to level spacing distributions of GOE and PS.

$p \ll 1$ it has the semi-Poisson level statistics $\mathcal{P}_{h=1}^{\beta=1}$. The bulk of the level spacing distribution of such an ensemble will be very close to the Wigner distribution $P_{\text{GOE}}(s)$ of the GOE matrix ensemble (as $p \ll 1$). However, for large level spacings, the distribution will be dominated by exponentially decaying tail of the level spacing distribution $P(s)$ from the small fraction of matrices with semi-Poisson statistics. Analogously, the number variance $\Sigma^2(L)$ will be a sum of logarithmically growing number variance for GOE and linearly increasing number variance for semi-Poisson statistics. Hence, it will be dominated by the latter and increase linearly with L with a very good approximation.

This leads us to a question whether the intersample randomness can be responsible for the exponential tails of level spacing distribution and a linear number variance in the MBL transition via the mechanism described above. To verify this, we examine level statistics of XXZ system at certain disorder strength but accept only disorder realizations for which the r_S belongs to a certain narrow interval—results for $W = 2.5$ are presented in Fig. 4. The procedure of selecting r_S affects significantly the resulting level statistics. As the interval of r_S shifts towards smaller values of r_S one obtains level spacing distributions with weaker and weaker level repulsion characterized by decreasing β and with growing weight of the exponential tail. Both features are precisely the asymptotic characteristics of the level spacing distribution for SRPM (9) for appropriately chosen β and h . However, our goal is to reproduce the full level statistics. An appropriate model should thus combine the contributions from disorder realizations with different localization properties reflected by the varying value of r_S .

This leads us to the formulation of the weighed short-range plasma model (wSRPM) which, by definition, has JPDF given by

$$P_{\text{wSRPM}}(E_1, \dots, E_N) = \sum_i c_i \mathcal{P}_{\beta_i}^{\beta_i}(E_1, \dots, E_N) \quad (11)$$

where h_i and β_i range over an appropriate set of values and c_i are weight coefficients ($\sum_i c_i = 1$). The weight

coefficients are determined by the requirement that the wSRPM reproduces the intersample randomness reflected by the $P(r_S)$ distribution. By integrating the JPDF for wSRPM with $\delta(s - |E_k - E_{k-1}|)$, one gets the level spacing distribution

$$P_{\text{wSRPM}}(s) = \sum_i c_i P_{\beta_i}^{\beta_i}(s), \quad (12)$$

which is a linear combination of the level spacing distributions $P_{\beta_i}^{\beta_i}(s)$. An analogous expression holds for the number variance

$$\Sigma_{\text{wSRPM}}^2(L) = \sum_i c_i \Sigma_{\beta_i, h_i}^2(L), \quad (13)$$

which stems from the formula $\Sigma^2(L) = L - \int_0^L dE(L - E)(1 - R_2(E))$ and the fact that the two-level correlation function $R_2(E)$ for wSRPM is a linear combination of two-level functions of SRPMs $\mathcal{P}_{\beta_i}^{\beta_i}$.

V. LEVEL SPACING DISTRIBUTION AND NUMBER VARIANCE ACROSS THE MBL CROSSOVER

The wSRPM model, defined by (11) depends on a large number of parameters, one needs to specify JPDFs of the SRPMs $\mathcal{P}_{\beta_i}^{\beta_i}$ which contribute to the full JPDF of the generalized model $\mathcal{P}_{\text{wSRPM}}$ and find appropriate weight coefficients c_i . To complete this task, we utilize the $P(r_S)$ distributions which encode the intersample randomness across the MBL transition. Distributions of r_S for individual SRPMs $\mathcal{P}_{\beta_i}^{\beta_i}(r_S)$ are Gaussian centered around $\bar{r}_{\beta_i}^{h_i}$ which depends on h_i and β_i parameters. The corresponding distribution for wSRPM reads $P_{\text{wSRPM}}(r_S) = \sum_i c_i \mathcal{P}_{\beta_i}^{\beta_i}(r_S)$ and the set of parameters $\{h_i, \beta_i, c_i\}$ is fixed by the requirement that $P_{\text{wSRPM}}(r_S)$ reproduces the $P(r_S)$ distribution for a given physical model [in this case, XXZ spin chain (2)] most faithfully. To fulfill the requirement in a robust way, we select a sequence of coefficients $\{(\beta_i, h_i)\}$ with $\bar{r}_{\beta_i}^{h_i}$ covering the interval $r_S \in [0.386, 0.531]$ possibly uniformly, i.e., we choose

$$(\beta_i, h_i) = \begin{cases} (\frac{i}{100}, 1), & i \in [0, 10], \\ (\frac{i-8}{20}, 1), & i \in [11, 30], \\ (1, i-30), & i \in [31, 30 + h_{\max}], \end{cases} \quad (14)$$

where h_{\max} specifies the maximal range of interactions in the contributing SRPMs. The chosen set of coefficients (14) determines the family of wSRPM that can be obtained by various choices of the weight coefficients $\{c_i\}$. One way of finding the weight coefficients $\{c_i\}$ would be to choose a number of points r_j and solve the linear system of equations $P(r_S = r_j) = P_{\text{wSRPM}}(r_S = r_j)$ for the $\{c_i\}$ coefficients given that the function $P(r_S = r_j)$ as well as $\mathcal{P}_{\beta_i}^{\beta_i}(r_S)$ are known. If the number of the points r_j is equal to number of coefficients c_i , the solution is unique. Unfortunately, this linear problem is badly conditioned, small changes of positions of r_j modify drastically the solution $\{\tilde{c}_i\}$. In particular, it may happen that certain coefficient \tilde{c}_k is large and positive whereas the next one \tilde{c}_{k+1} is large negative which illustrates that further constraints should be imposed on $\{c_i\}$. Namely, the weight coefficients must be positive $c_i > 0$ and the differences between subsequent c_i should not be too large. This leads us to a fitting

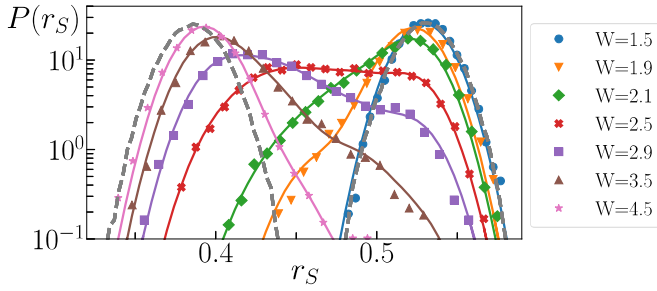


FIG. 5. The fit of $P(r_S)$ distributions. Distributions $P(r_S)$ of the sample-averaged gap ratio r_S for the XXZ spin chain Eq. (2) are denoted by markers. The corresponding wSRPM fits are denoted with solid lines. Gray dashed lines correspond to $P(r_S)$ for GOE and PS center, respectively, around $\bar{r}_{\text{GOE}} = 0.531$ and $\bar{r}_{\text{PS}} = 0.386$.

procedure which determines the weight coefficients $\{c_i\}$ by minimizing

$$\chi^2 = \sum_{i=0}^{i_{\max}} \frac{1}{m} (c_{i+1} - c_i)^2 + \int_{r_S^m}^{r_S^M} (P_{\text{wSRPM}}(r_S) - P(r_S))^2 dr_S. \quad (15)$$

The term $\sum_{i=0}^{i_{\max}} \frac{1}{m} (c_{i+1} - c_i)^2$ assures the “continuity” of c_i coefficients, the condition $c_i > 0$ becomes a constraint of the minimization procedure. The constant m is taken as 10^{-4} although changing it by a factor of 5 only mildly affects the results. Finally, the minimization of (15) does not resolve accurately SRPMs with large h as the spacing between subsequent \bar{r}_β^h decreases drastically, so that we take $h_{\max} = 5$ in (14).

Determining the constitutive SRPMs by the choosing the set $\{(\beta_i, h_i)\}$ according to (14) and specifying the method of obtaining the weight coefficients $\{c_i\}$, we defined a method of finding wSRPM which reproduces intersample randomness and can be used across the ergodic-MBL crossover.

A. Level statistics as a function of disorder strength

The distributions $P_{\text{wSRPM}}(r_S)$ found for the XXZ spin chain for varying disorder strength W for system of size $K = 16$ are presented in Fig. 5. Distributions $P(r_S)$ are indeed recovered in the whole crossover region. The distribution for $W = 1.5$, which is already very close to the GOE regime, is modeled by a single SRPM with $h = 12$ and $\beta = 1$.

Level statistics predicted by the wSRPM model together with XXZ spin chain (2) data across the MBL transition are presented in Fig. 6. We have accumulated data for $n = 2000$ disorder realizations for each disorder strength W and we have set the mean level spacing to unity (details described in the Sec. VII). The solid lines which denote the predictions of wSRPMs match with a very good accuracy both the bulks and the tails of level spacing distributions for disorder strengths W corresponding to the whole regime intermediate between GOE and PS level statistics. In particular, the tails of $P(s)$ for $W = 1.9, 2.1$ are visibly bent upwards—this is a clear manifestation that SRPMs which account for more localized rare events must be included in the wSRPM. The number variances $\Sigma^2(L)$ predicted by the wSRPM are again reproducing

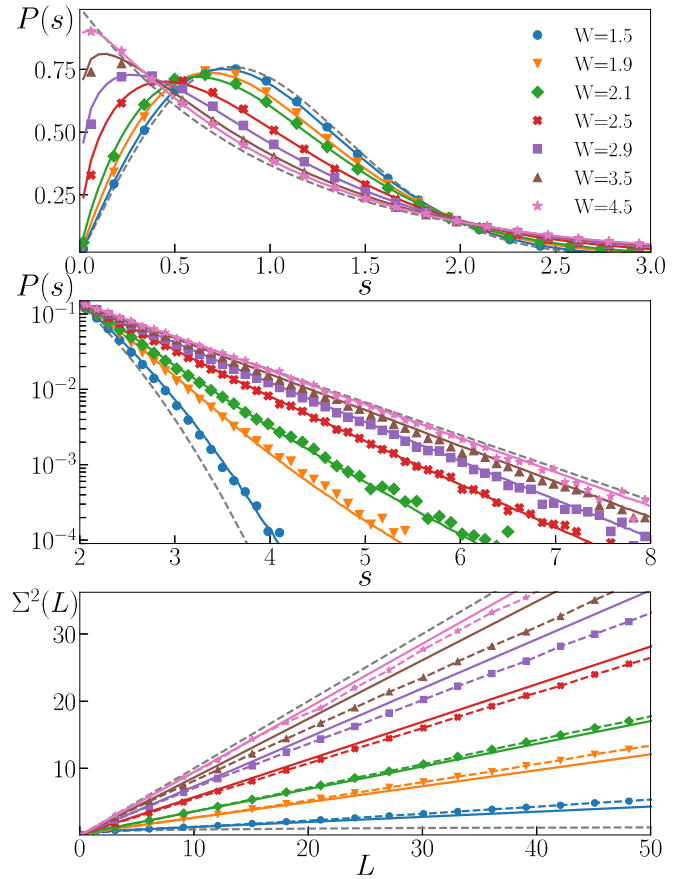


FIG. 6. (Top) Level spacing distributions $P(s)$ as a function of disorder strength W in XXZ spin chain (2) of size $K = 16$ are denoted by markers, wSRPM results denoted by solid lines and gray dashed lines denote the level spacing distributions in the limiting GOE and PS cases. (Middle) Same as above, but vertical axis in logarithmic scale to facilitate comparison between tails of level spacing distributions. (Bottom) Number variance $\Sigma^2(L)$ for XXZ spin chain (dashed lines with markers) and results for wSRPM model (solid lines). Gray dashed lines correspond to level spacing distribution or number variance for GOE and PS.

the data for XXZ spin chain (2) with a very good precision. The number variance predicted by fitting of a single SRPM presented in Fig. 3 was underestimating the result for $W = 1.9$ and it is the contribution from other SRPMs included in the wSRPM which ensures the agreement in the number variance.

Specific values of the weight coefficients are presented in Fig. 7. We also compare the mean gap ratio \bar{r} with the prediction of wSRPM $\bar{r}_{\text{wSRPM}} = \sum_i c_i \bar{r}_{\beta_i}^{h_i}$ in Table I showing the agreement at the level of 0.5%. In addition, we also collate spectral comprehensibilities. Predictions of wSRPM $\chi_{\text{wSRPM}} = \sum_i c_i / (h_i \beta_i + 1)$ agree with spectral comprehensibilities for XXZ spin chain obtained from quadratic fit to the number variance $\Sigma^2(L)$ for XXZ spin chain in the interval $L \in [10, 70]$ (see also Sec. VII) up to 10%.

B. Level statistics as a function of system size K

We have thus demonstrated that by constructing appropriate wSRPMs one can model flow of level statistics

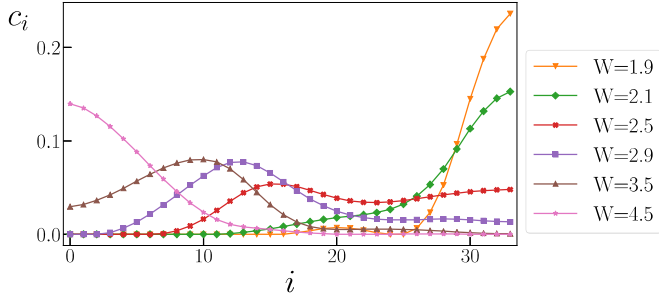


FIG. 7. Coefficients c_i for the wSRPM for XXZ spin chain across the ergodic-MBL crossover.

across the ergodic-MBL crossover for XXZ spin chain at given system size. In the following section, we demonstrate how the level statistics evolve with system size K for fixed disorder strength W .

A quick glance at Table II reveals the average gap ratio \bar{r} tends towards \bar{r}_{GOE} and \bar{r}_{PS} values with increasing system size K at disorder strengths close either to the ergodic regime ($W = 2.1$) or to the MBL phase ($W = 4.0$). The system size dependence is much stronger in the former case than in the latter as it is also visible in Fig. 8. The evolution of level spacing distribution $P(s)$ and number variance $\Sigma^2(L)$ with increasing system size is presented in Fig. 9. The level spacing and the number variance change with increasing size as the gap ratio suggest flowing either to GOE or to PS limit. The wSRPM determined by the requirement of reproducing the $P(r_s)$ distributions shown in Fig. 8 captures accurately level spacing distribution as well as the number variance for the considered system sizes. The evolution of parameters of the model with increasing system size is presented in Fig. 10 showing clearly that the weight of SRPMs closer to the GOE (those with larger i) increases with the growing system size. Analogous (albeit weaker) dependence is observed also close to the MBL regime ($W = 4.0$).

C. Flow of level statistics in the ergodic-MBL crossover

We have shown that wSRPM accurately describes level statistics of disordered XXZ spin chain across the whole ergodic to MBL crossover. The agreement is remarkably good even for long-range spectral correlations as shown by the number variance $\Sigma^2(L)$. This leads us to conclusion that

TABLE I. Values of the mean gap ratio \bar{r} and spectral compressibility χ for XXZ spin chain are compared with predictions of wSRPM model: \bar{r}_{wSRPM} and χ_{wSRPM} .

W	\bar{r}	χ	\bar{r}_{wSRPM}	χ_{wSRPM}
1.5	0.5306	0.0975	0.5282	0.078
1.9	0.5219	0.259	0.5189	0.238
2.1	0.5092	0.358	0.5074	0.338
2.5	0.4720	0.523	0.4719	0.562
2.9	0.4390	0.638	0.4384	0.711
3.5	0.4107	0.774	0.4101	0.850
4.5	0.3938	0.857	0.3941	0.929

TABLE II. Values of the mean gap ratio \bar{r} and spectral compressibility χ for XXZ spin chain are compared with predictions of wSRPM model: \bar{r}_{wSRPM} and χ_{wSRPM} .

	\bar{r}	χ	\bar{r}_{wSRPM}	χ_{wSRPM}
$W = 2.1$				
$K = 14$	0.4956	0.392	0.4946	0.432
$K = 16$	0.5092	0.354	0.5074	0.338
$K = 18$	0.5221	0.259	0.5193	0.231
$W = 4.0$				
$K = 14$	0.4021	0.743	0.4024	0.888
$K = 16$	0.3996	0.805	0.3992	0.905
$K = 18$	0.3989	0.849	0.3981	0.910

the effective interactions between eigenvalues in the MBL crossover are accurately grasped by level correlations of wSRPM.

The picture of the flow of level statistics from GOE to PS in the MBL transition which emerges is the following. In the ergodic phase the range of interactions between eigenvalues tends to infinity, $h = \max\{h_i\} \rightarrow \infty$, and the level statistics reduces to GOE case. As the disorder strength increases, the range of interactions between eigenvalues h declines to a finite value, level spacing distribution acquires an exponential tail and a finite spectral compressibility χ appears as the number variance grows linearly $\Sigma^2(L) \propto \chi L$. Upon further increase of the disorder strength, the range of interactions h decreases further. A larger contribution of level statistics with short-range interactions appears as it is visible in tails of level spacing distributions and in the enhancement of spectral compressibility χ . As the MBL phase is approached the interactions become local $h = 1$ and parameter $\beta = \max\{\beta_i\}$ starts to flow from $\beta = 1$ to $\beta = 0$ in the MBL phase similarly as in the second stage of the flow described in Ref. [35]. This final stage of the flow is also accompanied by rare inclusions of systems which have nearly ergodic properties as it is visible in the $P(r_s)$ distribution in Fig. 5. The presence of this contribution also slightly diminishes the number variance.

Level statistics on the ergodic side of crossover flow towards GOE limit for growing system size. Similarly, for disorder strength $W \gtrsim 4.0$ system approaches the PS limit as its size increases. The transition becomes sharper and the

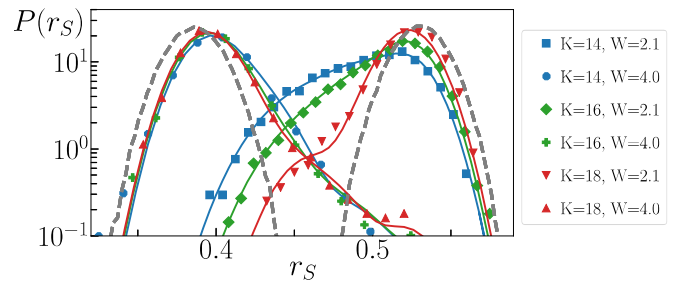


FIG. 8. The fit of $P(r_s)$ distributions. Distributions $P(r_s)$ of the sample-averaged gap ratio r_s for the XXZ spin chain Eq. (2) are denoted by markers. The corresponding wSRPM fits are denoted with solid lines. Gray dashed lines correspond to $P(r_s)$ for GOE and PS center, respectively, around $\bar{r}_{\text{GOE}} = 0.531$ and $\bar{r}_{\text{PS}} = 0.386$.

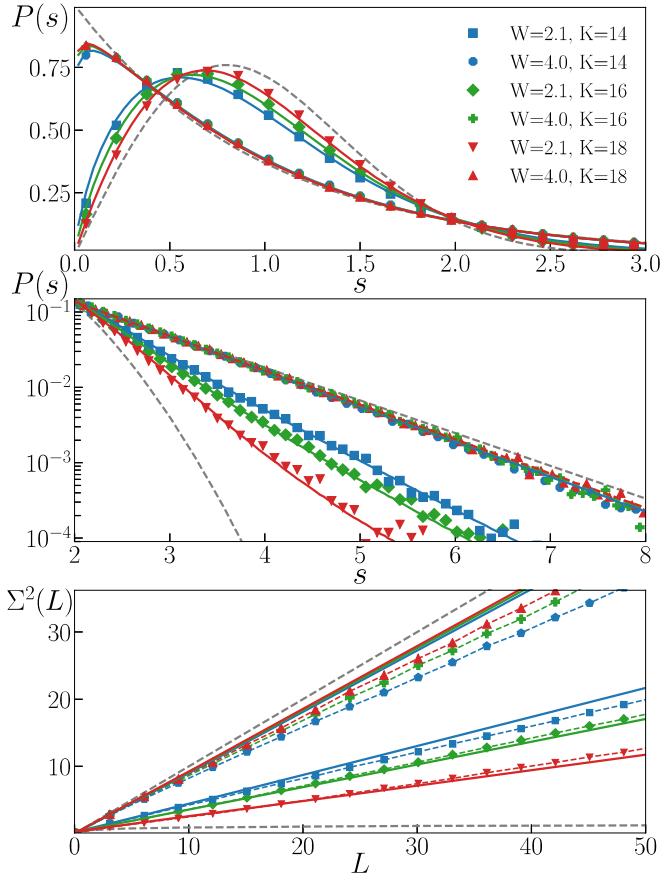


FIG. 9. (Top) Level spacing distributions $P(s)$ in XXZ spin chain (2) for varying system size K are denoted by markers, wSRPM results denoted by solid lines and gray dashed lines denote the level spacing distributions in the limiting GOE and PS cases. (Middle) Same as above, but vertical axis in logarithmic scale to facilitate comparison between tails of level spacing distributions. (Bottom) Number variance $\Sigma^2(L)$ for XXZ spin chain (dashed lines with markers) and results for wSRPM model (solid lines). Gray dashed lines correspond to level spacing distribution or number variance for GOE and PS.

range of disorder strengths W for which a wSRPM with more than a single nonzero coefficient shrinks with increasing system size. We speculate that in the $K \rightarrow \infty$ limit only at the critical disorder strength W_C the level statistics is neither GOE

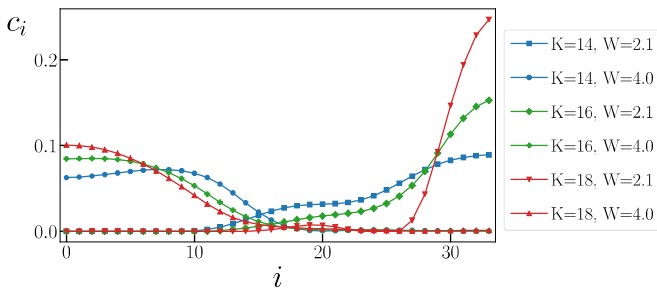


FIG. 10. Coefficients c_i for the wSRPM for XXZ spin chain for varying system size on the two sides of the ergodic-MBL crossover.

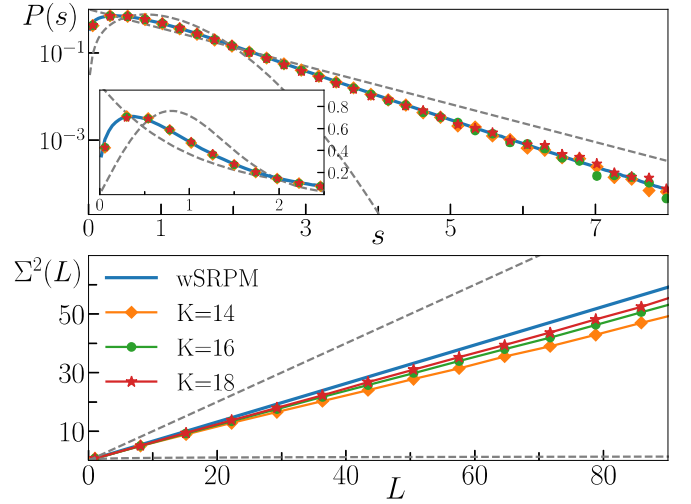


FIG. 11. Critical level statistics for XXZ spin chain with random uniform disorder. Dashed lines correspond to the GOE and Poisson cases.

nor PS. Candidate for such critical level statistics for the MBL transition is discussed in Sec. VD.

In conclusion, the wSRPM allows to model the level statistics in the XXZ spin chain in the whole MBL crossover. The level statistics are reproduced with a nearly perfect agreement on the level of ten level spacings. Slight discrepancies associated with long-range spectral correlations are discussed in Sec. VII. Now, we proceed to discussion of the critical level statistics in Sec. VD to further demonstrate that wSRPM describes also statistics observed for other systems that reveal MBL transition in Sec. VI.

D. Critical level statistics in MBL transition

We assume that the critical level statistics in MBL transition can be extracted from data for a system of size K for disorder strength W_K that maximizes the intersample variance V_s , e.g. $W_K = 2.7$ for $K = 16$. The finite size analysis assures that in the thermodynamic limit $K \rightarrow \infty$: $W_K \rightarrow W_C = 3.5(1)$ (as discussed in Sec. II).

As the system size increases the statistics on the ergodic (MBL) side of crossover tend towards GOE (Poisson) limit, the width of the crossover diminishes. The critical level statistics which we conjecture to be relevant exactly at the MBL transition in large system size limit is presented in Fig. 11. The obtained wSRPM contains SRPMs with long-range interactions $h > 1$ (nonzero weights c_i with $i > 30$) together with dominating contribution of models with local interactions and $\beta < 1$. Large number of contributing SRPMs allows to accurately reproduce the $P(s)$ distribution (Fig. 12). Moreover, it is vital to faithfully reproduce the number variance. The values of spectral compressibility χ defined by the linear large L behavior of the number variance $\Sigma^2(L) \propto \chi L$ together with the average gap ratios \bar{r} are shown in Table III. This quantities are in good agreement with the predictions of the wSRPM \bar{r}_{wSRPM} and χ_{wSRPM} . The data suggest that the remaining small deviation in the spectral compressibility χ is probably a finite size effect.

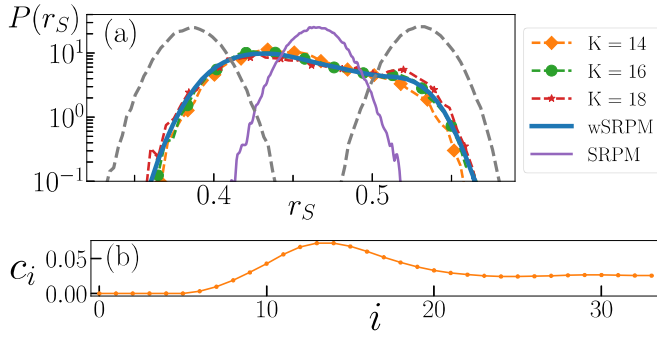


FIG. 12. (a) The $P(r_S)$ distribution for the critical statistics in XXZ spin chain along with wSRPM and $P(r_S)$ for SRPM. (b) The c_i coefficients of wSRPM shown in Fig. 11.

Level spacing distribution $P_A(s)$ in the Anderson transition [20] combines level repulsion at small s characteristic for GOE and an exponential tail of Poisson level statistics, the critical statistics shown in Fig. 11 also possess the two features. However, the large intersample randomness encoded in broad $P(r_S)$ distribution is a crucial property of the critical level statistics in MBL transition, whereas it does not play a role in the Anderson transition in which the $P_A(r_S)$ distribution has a Gaussian shape the same width as in the GOE and Poisson limits.

VI. UNIVERSALITY

The wSRPM model has so far been used to describe level statistics in the standard model of MBL—the XXZ spin chain (2). It has already been noted in Ref. [58] that there are differences in level statistics across the MBL transition in systems of hard-core bosons and fermions. In this section, we demonstrate that wSRPM can faithfully reproduce level statistics in ergodic to MBL crossover in a disordered Bose-Hubbard model [47] as well as in disordered Fermi-Hubbard model [42].

The system of disordered bosons is described by the Bose-Hubbard Hamiltonian

$$H_B = -J \sum_{\langle i,j \rangle} \hat{a}_i^\dagger \hat{a}_j + \frac{U}{2} \sum_i \hat{n}_i(\hat{n}_i - 1) + \sum_i \mu_i \hat{n}_i, \quad (16)$$

where \hat{a}_i^\dagger and \hat{a}_i are bosonic creation and annihilation operators, respectively, the tunneling amplitude $J = 1$ sets the energy scale, U is interaction strength, and the chemical

TABLE III. The average gap ratio \bar{r} and spectral compressibility χ for the XXZ spin chain at disorder strength which corresponds to W_C at in the thermodynamic limit $K \rightarrow \infty$. For comparison, the predictions of wSRPM r_{wSRPM} and χ_{wSRPM} are displayed.

K	W	\bar{r}	χ
14	2.62	0.4528(4)	0.545(9)
16	2.7	0.4537(5)	0.587(5)
18	2.8	0.4569(7)	0.605(4)
		\bar{r}_{wSRPM}	χ_{wSRPM}
		0.4530	0.639

potential μ_i is distributed uniformly in an interval $[-W; W]$. This model have been shown to be MBL [47] above a critical disorder strength W_B , which depends on the interaction strength U . The Hamiltonian for disordered fermions reads

$$H_{F0} = -J \sum_{i,\sigma=\uparrow,\downarrow} (\hat{c}_{i,\sigma}^\dagger \hat{c}_{i+1,\sigma} + \text{H.c.}) + U \sum_i n_{i\uparrow} n_{i\downarrow} + \sum_i \mu_i \hat{n}_i, \quad (17)$$

where $\hat{c}_i^\dagger \hat{c}_i$ are fermionic creation and annihilation operators, respectively; $J = 1$ and U are tunneling and interaction amplitudes and $\mu_i \in [-W; W]$ is uncorrelated disorder. To avoid integrability in the absence of disorder it is sufficient [42] to add the next-to-nearest neighbor tunneling terms

$$H_1 = -J' \sum_{i,\sigma} (\hat{c}_{i,\sigma}^\dagger \hat{c}_{i+2,\sigma} + \text{H.c.}) \quad (18)$$

and an additional symmetry breaking term

$$H_{SB} = h_B(n_{i\uparrow} - n_{i\downarrow}) + \mu_B(n_{L\uparrow} + n_{L\downarrow}). \quad (19)$$

Transition between GOE and PS statistics for the system with the full Hamiltonian

$$H_F = H_{F0} + H_1 + H_{BS} \quad (20)$$

has been observed in Ref. [42].

Level statistics as a function of disorder strength in the bosonic (16) and fermionic (20) models together with wSRPM fits are presented in Fig. 13. Similarly as in the case of XXZ spin chain, the level spacing distributions $P(s)$ are characterized by exponential tails (which are also bending upwards for large s), the number variance $\Sigma^2(L)$ is growing linearly at large L similarly as in the case of disordered XXZ chain. It seems that these are universal features of level statistics in ergodic to MBL crossover in models with short-range interactions. Such systems host an extensive number of LIOMs. Presumably, the observed common features of level statistics across the MBL crossover are associated with the way in which the LIOMs get delocalized as the disorder strength decreases.

Predictions of wSRPM reproducing appropriate $P(r_S)$ distributions for both systems are denoted by solid lines in Fig. 13. In the case of the fermionic system, the method of determining the wSRPM model was exactly the same as for the XXZ spin chain, whereas for bosons we have also included SRPM with $\beta = 1$ and $h = 25$ (it has $\bar{r}_{\beta=1}^{h=25} = 0.5302$ which can be compared with $\bar{r}_{\beta=1}^{h=5} = 0.5262$). For the smallest disorder strengths $W = 8.5$ ($W = 4.5$) for bosons (fermions), a single SRPM with $h = 12$ ($h = 13$) was fitted. The bulks of level spacing distributions as well as the tails are reproduced reasonably accurately by the wSRPM across the whole MBL crossover. The wSRPM prediction for the number variance $\Sigma^2(L)$ is compatible with data for disordered Fermi-Hubbard model. However, the number variance is significantly 20%–30% overestimated for the disordered Bose-Hubbard model at $W = 10$ and 12. Inspecting closely the $P(r_S)$ distributions in Fig. 14, we can clearly see abundance of disordered realizations with $r_S \gtrsim 0.57$ for $W = 10$ and 12 such that $P(r_S)$ is above the GOE distribution. Precisely this abundance lead us to consider also the $\beta = 1$ and $h = 25$ SRPM in the fits for bosonic system. While it diminishes the deviation of the number variance, it is clearly insufficient

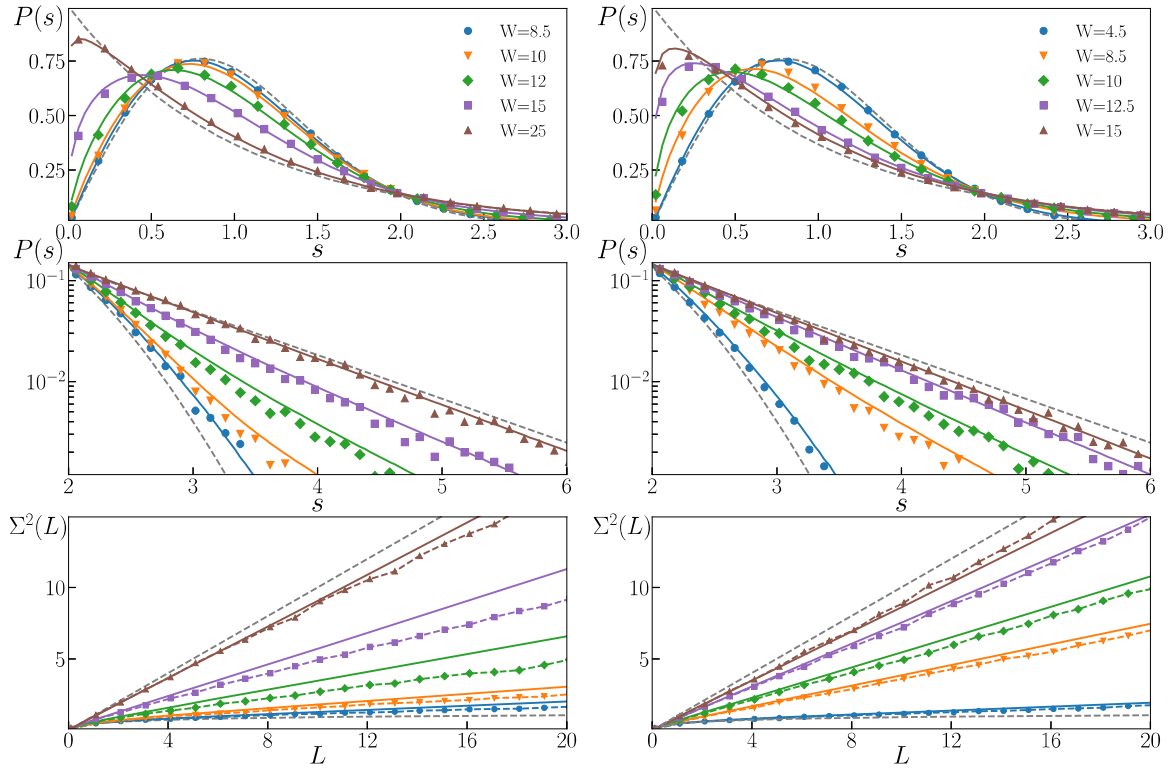


FIG. 13. (Left) Level spacing distribution $P(s)$ (in lin-lin and in lin-log scales) together with number variance $\Sigma^2(L)$ during MBL transition in disordered Bose-Hubbard model (16). Results for $N = 12$ bosons on $K = 8$ lattice sites, interaction amplitude $U = 1$ are denoted by markers, solid lines show wSRPM model fits. (Right) Level statistics for the Fermi-Hubbard model H_F . Results for $N_\uparrow = 3 = N_\downarrow$ fermions on $K = 12$ lattice sites with interaction strength $U = 2$ and $\mu_B = h_B = 0.1$, $J' = 0.5$ are denoted by markers, solid lines correspond to wSRPM model predictions.

to yield correct spectral compressibility. This demonstrates model specific long-range correlations between eigenvalues that cannot be grasped straightforwardly by wSRPM.

Apart from the model specific details, the exponential tails of level spacing distributions and the finite spectral compressibility that appear already deeply in the metallic phase were observed for the XXZ spin chain as well as in the bosonic and fermionic systems. The wSRPM model is able to grasp all of those features which provides an argument in favor of its generality. Moreover, distinct numbers of rare events occur in various systems during MBL transition which reveals itself in dissimilar correspondences between the bulk of level spacing distribution and its tail as well as the number variance. In general, different systems are characterized by different inter-

sample randomness during the MBL transition—compare for instance the shape of $P(r_s)$ distributions displayed in Fig. 14 with data for the XXZ spin chain in Fig. 5. This demonstrates that an accurate model of level statistics must be flexible enough to reproduce various types of intersample randomness across the MBL crossover; this necessitates an introduction of a weighted model like wSRPM.

VII. LONG-RANGE SPECTRAL CORRELATIONS

The number variance $\Sigma^2(L)$ at large L reflects correlations between energy levels which lie far apart in the spectrum of a system. Such long-range correlations between eigenvalues are strong in the GOE ensemble, resulting in the so called spectral rigidity which is apparent in the asymptotic behavior of the number variance $\Sigma_{\text{GOE}}^2(L) \rightarrow \ln(L)$ at $L \gg 1$. The spectral rigidity of GOE is associated with the fact that the logarithmic interactions act between all pairs of eigenvalues in the JPDF for GOE (7). And it is the spectral rigidity of β -Gaussian model which causes the large discrepancy between its prediction and the number variance for XXZ spin chain in Fig. 3. On the other hand, the SRPMs describe interactions only among a finite number h of neighboring eigenvalues which results in the spectral compressibility of those models $\Sigma_{\text{GOE}}^2(L) \rightarrow \chi L$ at $L \gg 1$, with $0 < \chi < 1$. The resulting spectral compressibility of the wSRPM model allows to grasp the linear behavior of number variance in the MBL crossover.

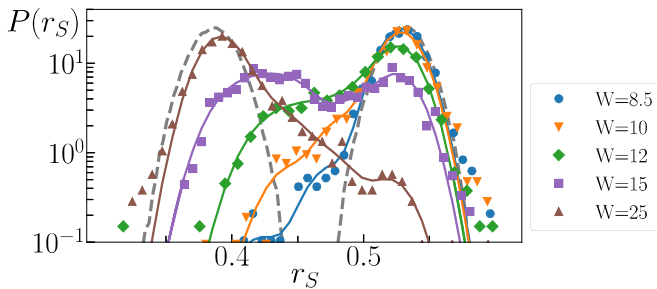


FIG. 14. The fit of $P(r_s)$ distributions. Data for bosonic system (16) are denoted with markers, solid lines show wSRPM fits.

The similar behavior can be also obtained with wPLRBM as presented in the preceding section.

To be able to compare statistical properties of eigenvalues from different parts of spectra of various systems, one has to perform the unfolding of energy levels [11]—the procedure of setting mean level spacing to unity. Unfortunately, the number variance $\Sigma^2(L)$ is very sensitive to details of the unfolding [59], which has already been a source of discrepancies in descriptions of level statistics in the MBL transition [35,36]. Consider a set of eigenvalues $\{E_i\}$ ordered in an ascending manner. During the unfolding, a level staircase function $\sigma(E) = \sum_i \Theta(E - E_i)$ is separated into smooth and fluctuating parts $\sigma(E) = \bar{\sigma}(E) + \delta\sigma(E)$ and the eigenvalues are mapped via

$$E_i \rightarrow \epsilon_i = \bar{\sigma}(E_i). \quad (21)$$

The difficulty of unfolding lies in an ambiguity of the definition of the smooth part $\bar{\sigma}(E)$ of the staircase function. The most common way is to fit the staircase function $\sigma(E)$ for each disorder realization with a polynomial of a small degree which determines the smooth part $\bar{\sigma}(E)$.

In our case, a set of $n = 400$ consecutive eigenvalues is gathered and the resulting level staircase is fitted with a straight line which defines the smooth part $\bar{\sigma}(E)$ used in the unfolding of energy levels. For each disorder realization, seven nonoverlapping sets of $n = 400$ eigenvalues from the middle of spectrum are taken—effectively employing $\approx 20\%$ of the spectrum to the analysis as the matrix size for $K = 16$ is equal to 12870. The finite size n of the set of eigenvalues introduces a correction $-a_2 L^2/n$ to the number variance [60]. Carrying out the unfolding with $n = 50, 100, 200, 400, 800$, we verify that it is indeed the case. We perform a quadratic fit to $\Sigma^2(L)$ in the interval $L \in [10, 70]$ and obtain the coefficient a_2 which is weakly dependent on the chosen L interval. Therefore, in order to eliminate the quadratic correction and thus to get rid of the finite n effects, we subtract the $-a_2 L^2/n$ term from the number variance data. Let us note that unfolding with finite number n of energy levels can have two consequences. For eigenvalues that are strongly correlated at large distances (e.g., GOE), it destroys level correlations at approximately n level spacings meaning that at this ranges the eigenvalues become uncorrelated. Hence, the number variance becomes overestimated at $L \approx n$. The converse is true for uncorrelated energy levels—unfolding based on n energy levels introduces correlations between them at a certain scale—and the number variance is underestimated. We have checked that our unfolding procedure (together with the $-a_2 L^2/n$ term subtraction) allows us to get correct number variances in the two limiting cases of GOE and PS statistics up to $L \approx 100$.

The number variances for the XXZ spin chain (2) at various disorder strengths W together with the wSRPM results from Sec. V A are presented in Fig. 15. Nearly perfect agreement between the XXZ spin chain data and the predictions of wSRPM visible in Fig. 6 for $L \in [0, 20]$ is lost. Small deviations from the linear behavior of the number variance predicted by wSRPM appear at larger scales which was also indicated by the slight discrepancies between spectral compressibility χ of the data and the prediction of wSRPM. There are two distinct regimes. For metallic systems with disorder strengths $W \lesssim 2.1$, the number variance obtained from the wSRPM is

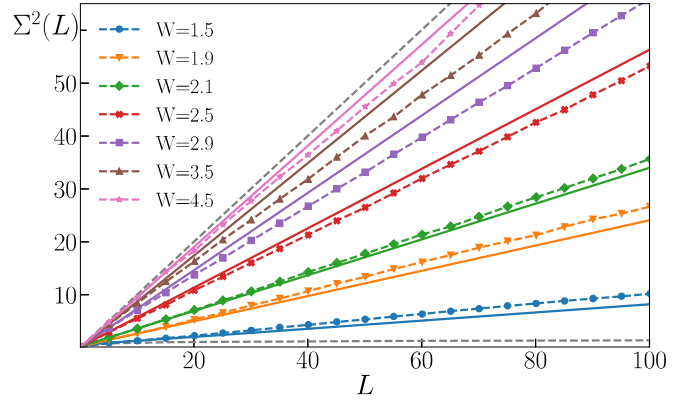


FIG. 15. Long-range spectral correlations visible in large L behavior of the number variance $\Sigma^2(L)$ for XXZ spin chain (2) during the MBL transition. The dashed lines denote predictions of the wSRPMs with parameters from Table I.

smaller than the result for XXZ spin chain. This indicates that there exists a regime (for $L \gtrsim 20$) where the number variance grows faster than linearly which was interpreted in Ref. [36] as a signature of anomalous Thouless energy in the system [61]. We indicate below that this behavior of the number variance for large L has to be examined with an uttermost caution. The second regime arises as the disorder strength increases above $W \approx 2.5$. Then, the number variance predicted by wSRPM slightly overestimates the number variance for the XXZ spin chain. As we have shown in Fig. 9, this effect diminishes as one changes the system size from $K = 14$ through $K = 16$ to $K = 18$ and thus it is likely a finite size effect. However, we cannot completely exclude the possibility that there are some remaining long-range correlations between eigenvalues in the system which are not grasped within the wSRPM.

The simple form of JPDF of wSRPM allows us to get further insight into long-range spectral correlations of system in the MBL crossover. The situation in which wSRPM accurately reproduces level statistics up to 10–20 level spacings but underestimates the number variance for $L \gtrsim 20$ is at first sight paradoxical. The wSRPM incorporates interactions between energy levels only at a finite range $h = \max\{h_i\}$. In addition, the weaker the correlation between eigenvalues separated by a given distance the bigger is the number variance at L corresponding to this distance. How it is, therefore, possible that wSRPM grasps faithfully the level statistics at the local scale but predicts stronger correlations at larger scales as compared to the data for the XXZ spin chain while at the same time it does not assume presence of any interactions between energy levels beyond the range h ? It turns out that fluctuations of density of eigenvalues on scales of tens level spacings increase the number variance at large L . This is precisely the moment in which the unfolding enters the scene as it is the way in which the $\bar{\sigma}(E)$ is defined which determines whether the density fluctuations are incorporated into $\bar{\sigma}(E)$ resulting in number variance $\Sigma^2(L)$ growing linearly with L (or, conversely, they are not incorporated and then $\Sigma^2(L)$ increases faster than linearly for large L). The work [36] reports that the number variance grows according to a power law $\Sigma^2(L) \propto L^\gamma$ with $\gamma > 1$ for large L for the XXZ spin chain

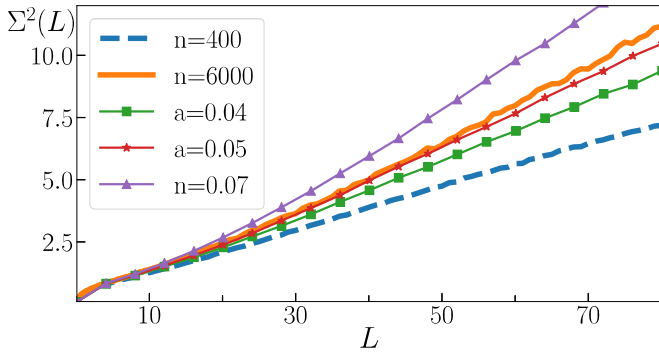


FIG. 16. The number variance $\Sigma^2(L)$ for XXZ spin chain (2) of size $K = 18$ for $W = 1.5$. The dashed line shows result for local linear unfolding with $n = 400$, the solid line for unfolding based on mean density of states [36] with $n = 6000$. The number variance $\Sigma^2(L)$ obtained after introducing of fluctuations of density of eigenvalues with parameter a are denoted with lines with markers.

(2) deep in the metallic regime where the exponent γ acquires values up to $\gamma \approx 1.4$. The number variance obtained by us for $W = 1.9$ has clearly some region in which it increases faster than linearly, but such a power-law growth is not observed by us. This discrepancy has its root in the unfolding. Unfolding employed in Ref. [36] relies on assumption that the shape of mean density of states obtained for the system at given disorder strength can be used (after appropriate linear transformations) to unfold large portions of spectrum of the system taking $n \approx 6000$ consecutive energy levels for $K = 18$. The fluctuations of density of eigenvalues on the scales of tens or hundreds of eigenvalues which are different for different disorder realizations are not incorporated in the $\bar{\sigma}(E)$ as it is determined by the mean density of states in which such fluctuations are averaged out.

Figure 16 compares the number variances obtained after the local linear unfolding with $n = 400$ consecutive eigenvalues and after the unfolding of Ref. [36]. The results agree up to $L \approx 15$. In order to show that the difference between the results stems from the density fluctuations, we introduce a particular density modulation to the data from the local linear unfolding. Namely, the unfolding is modified so that the eigenvalues are mapped via

$$E_i \rightarrow \epsilon_i = \bar{\sigma}(E_i) + a(E_i - E_C)^2, \quad (22)$$

where E_C lies in the middle of the energy interval which is unfolded. The $a(E_i - E_C)^2$ term mimics the density fluctuations which were not incorporated into $\bar{\sigma}(E)$, for $a = 0$ (22) reduces to the local linear unfolding (21). Such a density modulation does not alter $P(s)$ at all, however, it modifies the number variance exactly in the manner which allows us to reproduce the result of Ref. [36] and showing that the density fluctuations are the mechanism which causes the power-law growth of the number variance.

In conclusion, the behavior of the number variance $\Sigma^2(L)$ suggests that long-range spectral correlations might be present in the level statistics of XXZ spin chain during MBL transition. This feature of MBL transition lies beyond the scope of wSRPM, however, as we demonstrated by examining bosonic and fermionic systems it is model dependent. It is not clear

whether the unfolding employed in Ref. [36] is justified. As we have indicated, it does not take into account variations of density of eigenvalues at scales of tens and hundreds of level spacings for a given disorder realization. Let us emphasize once again that the situation of localization of an interacting system differs starkly from the usual RMT where a random matrix depends on number of random entries which scales as square of its size whereas the number of random entries in the Hamiltonian of the XXZ spin chain scales only as logarithm of the size of the Hilbert space of the system. Therefore one may expect that while the density fluctuations average out for RMT and using Wigner's semicircle to unfold GOE is a good idea it may not be the case for the many body quantum systems which undergo MBL transition.

VIII. CONCLUSIONS AND BEYOND

Analyzing the gap ratios of systems in the crossover between ergodic and many-body localized regimes we have shown that a complete information about inter- and intrasample randomness can be obtained from the r_n variables. Distribution $P(r_s)$ of the sample averaged gap ratio r_s provides a suggestive illustration of Griffiths regions in the case of random disorder while it shows absence of such rare events in systems with quasiperiodic disorder. The proposed inter- and intrasample variances V_s and V_l provide a straightforward method to quantify inter- and intrasample randomness. While our analysis provides further insights into role played by Griffiths regions in MBL transition, it is conceptually and computationally (involves only eigenvalues) simple and therefore can be straightforwardly employed in studies of other systems where a transition between integrable and RMT-like regimes occurs.

Examining the bulk and the tail of level spacing distribution together with the number variance, we have demonstrated that the proposed models of spectral statistics in MBL crossover [35,36,38,39] grasp level statistics accurately only at the level of few of level spacings. To reproduce broad distributions of the sample averaged gap ratio r_s in the MBL transition, we have introduced the wSRPM that is a statistical mixture of the well known family of short-range plasma models. The wSRPM describes faithfully the flow of level statistics in the whole ergodic to MBL crossover. According to wSRPM the correlations between eigenvalues are present only at a finite range h . In the ergodic phase the range h diverges resulting in GOE statistics and as the system flows towards MBL phase the range of correlations diminishes. At a certain point, the interactions become local ($h = 1$), finally in the vicinity of MBL phase the level repulsion vanishes ($\beta \rightarrow 0$) resulting in the Poisson statistics. The wSRPM grasps universal features of level statistics across MBL transition in a variety of spin, bosonic and fermionic systems with interactions and random disorder. The assumption that there are no correlations between eigenvalues at ranges larger than h predicts the finite spectral compressibility χ in the transition. The latter seems to be approximately true for the studied systems albeit small deviations from the linear behavior of the number variance have been noticed. This may be either an artifact of the unfolding procedure or could also stem from

TABLE IV. Coefficients, $h = 2$, $P(n, s) = \exp(-3s)s^{3n} \sum_j w_j s^j$.

	$n = 0$	$n = 1$	$n = 2$	$n = 3$	$n = 4$
w_1	2.4773	2.50542	0.325782	0.0160653	1.9203×10^{-4}
w_2	6.06811	3.0685	0.243833	6.51294×10^{-3}	8.2295×10^{-5}
w_3	3.71594	0.751625	4.0723×10^{-2}	6.0483×10^{-4}	8.2297×10^{-6}

weak long-range interactions between energy levels which are model and system size dependent.

We also considered a weighted ensemble of power law banded random matrices—see Appendix B. An appropriate mixture of PLBRM (again necessitated by a broad distribution of gap ratio in physical samples) seems to be at least competitive with wSRPM leading to small deviations of the fitted model from the data for XXZ spin chain. Both approaches have their advantages. While for SRPMs the eigenvalues may be generated by brute force Monte Carlo integration of the JPDP, a softer semi-analytic approach, working at certain range of eigenvalues interaction, h , is possible following the path shown by Bogomolny and coworkers [55] as shown in Appendix A. It provides expressions for the level spacing distribution $P(s)$ and, more importantly, gives analytical formulas for asymptotic behavior of the number variance $\Sigma^2(L)$ as well as for the tails of $P(s)$. Moreover, the wSRPM gives a concrete microscopic description of correlations between eigenvalues across the whole MBL crossover and allows us to speculate how the level statistics evolve in the limit of large system sizes.

On the other hand that approach provides us with no clue on the eigenvectors behavior. On the contrary, PLBRM model provides access to both eigenvalues and eigenvectors by a direct (although costly) diagonalization of a large number of matrices from the ensemble. The drawback of this approach is that there are no analytical results for this model at finite N or $\mu \neq 1$ so a clear picture of correlations between eigenvalues is not available.

Finally, it is also interesting to note that the MBL transition for the quasiperiodic disorder case cannot be described by the proposed weighted ensembles. It supports the claim of Ref. [33] that the transitions for RD and QPD are of different universality classes. The ensemble that reproduces level statistics for QPD in MBL transition is yet to be identified.

ACKNOWLEDGMENTS

We acknowledge fruitful and enlightening discussions with D. Delande as well as exchanges on unfolding procedures

with A. M. Garcia-Garcia and M. Sieber. This work was performed with the support of EU via Horizon2020 FET project QUIC (No. 641122). Numerical results were obtained with the help of PL-Grid Infrastructure. We acknowledge support of the National Science Centre (PL) via Project No. 2015/19/B/ST2/01028 (P.S.), No.2018/28/T/ST2/00401 (Etiuda scholarship—P.S.) and the QuantERA programme No. 2017/25/Z/ST2/03029 (J.Z.).

APPENDIX A: ANALYTICAL EXPRESSIONS FOR SHORT-RANGE PLASMA MODEL

The following quantities are needed in order to construct wSRPM: level spacing distributions $P_h^\beta(s)$, number variances $\Sigma_{\beta,h}^2(L)$, the sample gap ratio distribution $P_h^\beta(r_s)$ of the individual SRPMs used in the wSRPM. Semianalytic expression for most of those quantities have been given in Ref. [55]. We comment here on how they can be used in the context of wSRPM.

Let us start with $h = 1$. The distribution of level spacing between n th neighboring eigenvalues reads

$$P_{h=1}^\beta(n, s) = \frac{(\beta + 1)^{(n+1)(\beta+1)}}{\Gamma((\beta + 1)(n + 1))} s^{\beta+n(\beta+1)} e^{-(\beta+1)s}, \quad (\text{A1})$$

where $\beta \in [0, 1]$, for $n = 0$ this distribution reduces to the usual level spacing distributions. For $n \geq 0$, formula (A1) can be used to obtain the number variance according to the following general expression:

$$\Sigma^2(L) = L - 2 \int_0^L ds (L - s) \left(1 - \sum_{n=0}^{\infty} P(n, s) \right). \quad (\text{A2})$$

From our Monte Carlo evaluation of JPDP (8), we know that the $P_h^\beta(r_s)$ distributions (for range h and β relevant in applications of our wSRPM) are Gaussian functions, localized around certain values \bar{r}_h^β with standard deviation $\sigma \approx 0.01557$, which changes only very slightly for various h and β . Therefore, instead of deriving the full $P_{h=1}^\beta(r_s)$ distribution, we simply use the distribution of gap ratio to calculate $\bar{r}_{h=1}^\beta$

TABLE V. Coefficients, $h = 3$, $P(n, s) = \exp(-4s)s^{4n-1+\delta_{0,n}} \sum_j w_j s^j$, where $\delta_{i,j}$ denotes the Kronecker delta.

	$n = 0$	$n = 1$	$n = 2$	$n = 3$	$n = 4$
w_1	2.13422	1.13398	0.14101	3.03041×10^{-3}	1.7921×10^{-5}
w_2	7.81963	3.63343	0.29749	4.48832×10^{-3}	2.0107×10^{-5}
w_3	11.6945	5.01886	0.26416	2.81378×10^{-3}	9.7956×10^{-6}
w_4	9.07429	3.71122	0.12338	9.58731×10^{-4}	2.6381×10^{-6}
w_5	3.68554	1.50368	3.2011×10^{-2}	1.87245×10^{-4}	4.1257×10^{-7}
w_6	0.62587	0.310017	4.455×10^{-3}	2.00989×10^{-5}	3.5835×10^{-8}
w_7	0	2.59412×10^{-2}	2.6414×10^{-4}	9.37094×10^{-7}	1.3637×10^{-9}

TABLE VI. Coefficients, $h = 4$, $P(n, s) = \exp(-5s)s^{(n+1)(n+4)/2-2} \sum_j w_j s^j$.

	$n = 0$	$n = 1$	$n = 2$	$n = 3$
w_1	1.9869	0.810475	0.0483296	7.29136×10^{-4}
w_2	9.44665	3.61582	0.190586	2.12001×10^{-3}
w_3	20.1982	7.54195	0.351477	2.85649×10^{-3}
w_4	25.6905	9.67193	0.399671	2.35667×10^{-3}
w_5	21.5383	8.44298	0.310511	1.32441×10^{-3}
w_6	12.39	5.24733	0.172672	5.34180×10^{-4}
w_7	4.90293	2.35889	7.01559×10^{-2}	1.58784×10^{-4}
w_8	1.28897	0.763259	2.0934×10^{-2}	3.51389×10^{-5}
w_9	0.204419	0.17333	4.55485×10^{-3}	5.76574×10^{-6}
w_{10}	0.0148948	2.61995×10^{-2}	7.06631×10^{-4}	6.86517×10^{-7}
w_{11}	0	2.36573×10^{-3}	7.44424×10^{-5}	5.64602×10^{-8}
w_{12}	0	9.63045×10^{-5}	4.79282×10^{-6}	2.87566×10^{-9}
w_{13}	0	0	1.42564×10^{-7}	6.85001×10^{-11}

and use the Gaussian approximation for the full distribution $P_{h=1}^\beta(r_s)$. The gap ratio distribution $P_{h=1}^\beta(r)$ reads [62]

$$P_{h=1}^\beta(r) = \frac{\Gamma(2\beta+2)\Gamma^2(\beta+2)}{(\beta+1)^2\Gamma^4(\beta+1)} \frac{2r^\beta}{(1+r)^{2\beta+2}}, \quad (\text{A3})$$

from which we get $\bar{r}_{h=1}^\beta$ as the first moment of $P_{h=1}^\beta(r)$ distribution.

For $h > 1$, the only interesting case for us is $\beta = 1$. Then, the level spacing distribution is given by (9). In order to determine the polynomial $W(s)$ as well as the distributions $P_h^\beta(n, s)$ for $h > 1$ and $n > 0$, one needs to solve the integral equation [55]

$$\begin{aligned} \int_0^\infty d\xi_h e^{-\xi_h} \xi_h (\xi_h + \xi_{h-1}) \dots (\xi_h + \dots + \xi_1) \psi_j(\xi_2, \dots, \xi_h) \\ = \lambda_j \psi_j(\xi_1, \dots, \xi_{h-1}), \end{aligned} \quad (\text{A4})$$

for function $\psi_j(\xi_1, \dots, \xi_{h-1})$. The equation can be solved by a polynomial ansatz

$$\begin{aligned} \psi_j(\xi_1, \dots, \xi_{h-1}) \\ = \sum_{i_1=0}^1 \sum_{i_2=0}^3 \dots \sum_{i_{h-1}=0}^{(h-1)h/2} a_{i_1 i_2 \dots i_{h-1}} \xi_1^{i_1} \xi_2^{i_2} \dots \xi_{h-1}^{i_{h-1}}, \end{aligned} \quad (\text{A5})$$

which reduces (A4) to an eigenproblem for a matrix of dimension $D_h = \prod_{k=1}^{h-1} i_k$. Solving the eigenproblem, the eigenfunctions $\psi_j(\xi_1, \dots, \xi_{h-1})$ can be used to find $P_h^\beta(n, s)$ for $h > 1$ and $n \geq 0$ as well as $P_h^\beta(r)$ which is then used to determine $P_h^\beta(r_s)$ as a Gaussian function with standard deviation $\sigma = 0.01557$ centered around \bar{r}_h^β . The level spacing distribution is determined as $P_h^\beta(s) = P_h^\beta(n=0, s)$, whereas $P_h^\beta(n=0, s)$ for $5 > n \geq 0$ are used to find the number variance $\Sigma_{\beta,h}^2(L)$

TABLE VII. Coefficients, $h = 5$, $P(n, s) = \exp(-6s)s^{(n+1)(n+4)/2-2} \sum_j w_j s^j$.

	$n = 0$	$n = 1$	$n = 2$	$n = 3$
w_1	1.90607	0.6725112	2.816938×10^{-2}	1.90849×10^{-4}
w_2	11.0655	3.757313	0.1474950	8.91886×10^{-4}
w_3	30.0426	10.08246	0.37248642	2.00465×10^{-3}
w_4	50.783	17.24174	0.60284124	2.87998×10^{-3}
w_5	59.9035	21.02683	0.70045560	2.96413×10^{-3}
w_6	52.2919	19.39166	0.62020	2.32137×10^{-3}
w_7	34.9026	13.99334	0.43344442	1.43410×10^{-3}
w_8	18.1222	8.06393	0.2443500	7.15049×10^{-4}
w_9	7.36415	3.75359	0.11260234	2.92059×10^{-4}
w_{10}	2.33283	1.41789	4.27332×10^{-2}	9.8650×10^{-5}
w_{11}	0.567501	0.4341132	1.339465×10^{-2}	2.77077×10^{-5}
w_{12}	0.102858	0.1069601	3.464275×10^{-3}	6.48527×10^{-6}
w_{13}	4.05358×10^{-5}	2.09130×10^{-2}	7.357053×10^{-4}	1.26372×10^{-6}
w_{14}	0	3.17047×10^{-4}	1.271140×10^{-4}	2.04088×10^{-7}
w_{15}	0	3.59091×10^{-4}	1.760258×10^{-5}	2.70805×10^{-8}
w_{16}	0	2.85564×10^{-6}	1.908644×10^{-6}	2.908829×10^{-9}
w_{17}	0	1.41936×10^{-6}	1.561970×10^{-7}	2.44768×10^{-10}
w_{18}	0	3.30973×10^{-8}	9.07438×10^{-9}	1.62366×10^{-11}
w_{19}	0	0	3.33532×10^{-10}	5.17973×10^{-13}
w_{20}	0	0	5.82950×10^{-12}	1.11711×10^{-12}

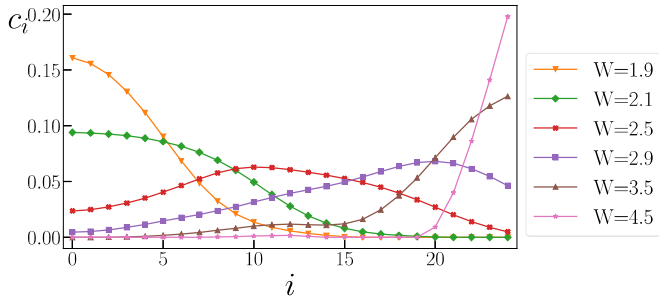


FIG. 17. Coefficients c_i for the wPLRBM model for XXZ spin chain across the ergodic MBL crossover.

for $L < 3$. For larger values $L \geq 3$, the asymptotic form (10) of the number variance is used.

Unfortunately, the dimension D_h grows exponentially with h which makes the semi-analytic approach feasible only for $h < 6$, which incidentally covers all the SRPMs used in (14). The coefficients which determine $P_h^\beta(n, s)$ are gathered in Tables IV–VII. The $P_h^{\beta=1}(r_s)$ distributions are approximated as Gaussian distributions with standard deviation $\sigma = 0.01557$ centered around the semianalytically obtained values of $\bar{r}_h^{\beta=1}$, which are 0.5155, 0.5206, 0.5231, 0.5246 for $h = 2, 3, 4, 5$, respectively.

APPENDIX B: WEIGHTED POWER-LAW RANDOM BANDED MATRICES

The wSRPM describes faithfully level statistics in MBL transition. However, it provides no information on properties of eigenstates. One particularly interesting property is multifractality of matrix elements of local operators [63,64] in such states. Therefore an identification of a random matrix model which could provide some information about eigenvectors in MBL transition can be productive.

In this Appendix, we examine an ensemble of power-law random banded matrices (PLRBM) [24,65] which is the ensemble of $N \times N$ symmetric real matrices with matrix elements H_{ij} being independent random Gaussian variables with

$$\langle H_{ij} \rangle = 0 \quad \text{and} \quad \langle H_{ij}^2 \rangle = (1 + \delta_{ij})(1 + (|i - j|/B)^{2\mu})^{-1}. \quad (\text{B1})$$

This ensemble interpolates between GOE statistics for $B \gg 1$, $\mu < 1$ and PS statistics which arises for $\mu > 1$ in $N \rightarrow \infty$ limit. In the special case of $\mu = 1$ and large B the model can

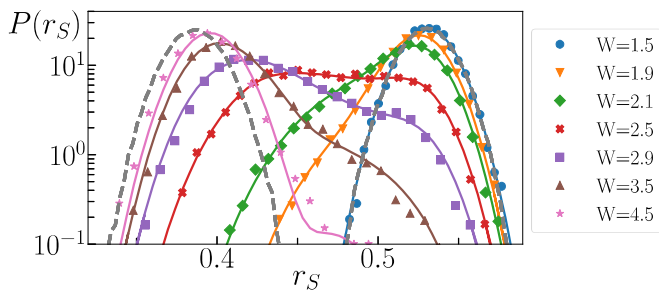


FIG. 18. Distributions $P(r_s)$ across the MBL transition (denoted by markers) with fits from the weighted PLRBM model.

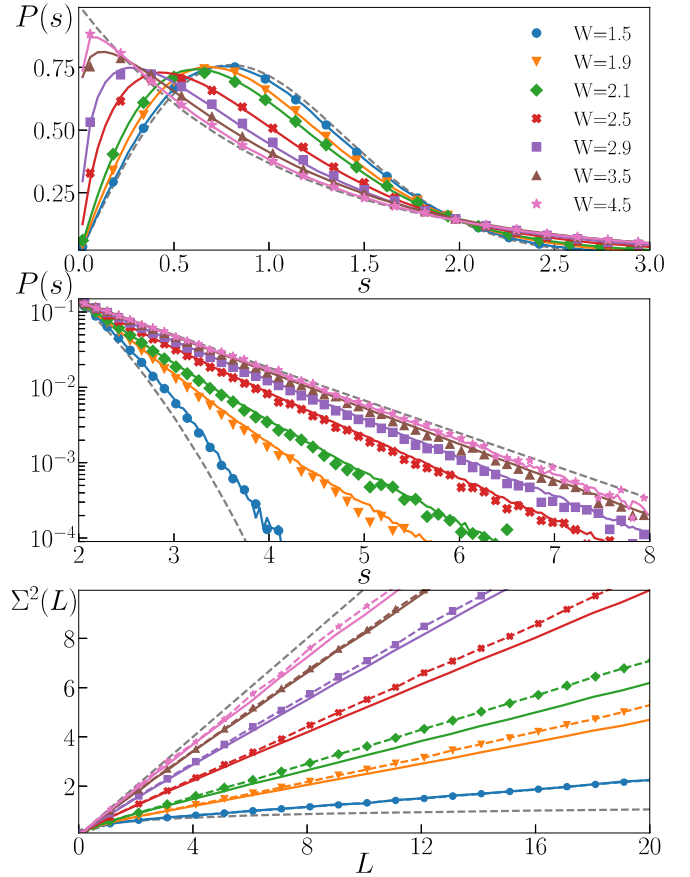


FIG. 19. Level statistics of XXZ spin chain fitted with wPLRBM model.

be solved by a mapping onto an effective σ model [66]. Numerical calculations of level statistics of the PLRBM model at the critical line $\mu = 1$ were carried out in Refs. [60,67].

We consider PLRBM of size $N = 1000$, accumulating 10 000 matrices for each set of parameters (μ, B) . Let us note that the exact values of the (μ, B) coefficients are strongly dependent on size N of matrix from PLRBM. With growing N a flow of level statistics in this model occurs—points (μ, B) with $\mu < 1$ correspond to statistics closer and closer to GOE and analogously—for $\mu > 1$ statistics flow towards PS. Calculating the $P(r_s)$ distribution for PLRBM model we have verified that $P(r_s)$ remains Gaussian in large region of parameter space (μ, B) . Moreover, there exist a region of parameters for which the level spacing distributions $P_B^\mu(s)$ decay exponentially and the number variance $\Sigma_{\mu, B}^2(L)$ is asymptotically linear. Therefore a similar extension as in the case of SRPM can be proposed in which the intersample randomness encoded in the $P(r_s)$ distribution is mimicked by considering a mixture of PLRBM with various μ_i and B_i to describe the level statistics in given point of MBL transition. More precisely, the selected set of PLRBMs consists of models with $B_i = 0.35$ and varying $\mu_i \in \{0.75 + i \times 0.025\}_{i=0,1,\dots,22,24,26,28,32,39,49}$. The corresponding weight coefficients are obtained by minimizing χ^2 as in (15) with results shown in Fig. 17 and in Fig. 18. The $W = 1.5$ was fitted with single PLRBM model with $B = 0.35$, $\mu = 0.7$.

Let us note that this model gives very good agreement at the level of tens level spacings as depicted in Fig. 19. Tails of the level spacing distributions as well as the number variance obtained from weighted PLRBM model are compatible with the XXZ spin chain data. Certain deviations are visible in the spectral compressibility χ at larger L .

The PLRBM model was introduced as a model for studies of critical properties of Anderson localization. In its direct interpretation, the model (B1) describes a single particle on one-dimensional sample with disorder and with long-range hopping—tunneling amplitude decays according to a power law with distance. Our results show that the PLRBM can be used also in MBL transition provided the weighted mixture of matrices is considered.

Such an ensemble needs to be introduced to mimic the large intersample randomness in the MBL crossover, which is a specific feature of localization of an interacting system, whose exponentially large in L Hamiltonian matrix depends only on L random variables.

One way of interpreting this result is that MBL can be thought of as a single-particle localization in a “Fock-space lattice” with complex geometry [68,69] (reflecting the quantum many-body character of the phenomenon). Another approach is to view wPLRBM as the Hamiltonian of the system at late stages of diagonalization flow [70–72] so that the diagonal entries represent random eigenenergies associated with soon-to-be LIOMs and the quickly decaying off-diagonal elements account for still present interactions which become weaker and weaker close to the MBL phase.

If the latter is true, then to get the multifractal properties of matrix elements of local operators [63,64] one has to know transformation between the σ_i^z eigenbasis (in which the Hamiltonian matrix is straightforwardly computed) and the basis in which the Hamiltonian becomes the banded matrix. This would also be the basis in which an interesting relation between the multifractal dimension D_1 and the spectral compressibility χ holds. This is beyond the scope of the present paper.

-
- [1] J. Wishart, *Biometrika* **20A**, 32 (1928).
 - [2] R. A. Janik and M. A. Nowak, *J. Phys. A: Math. Gen.* **36**, 3629 (2003).
 - [3] C. W. J. Beenakker, *Phys. Rev. Lett.* **70**, 1155 (1993).
 - [4] J. J. M. Verbaarschot and I. Zahed, *Phys. Rev. Lett.* **70**, 3852 (1993).
 - [5] Y. V. Fyodorov and H.-J. Sommers, *J. Math. Phys.* **38**, 1918 (1997).
 - [6] Y. V. Fyodorov and B. A. Khoruzhenko, *Phys. Rev. Lett.* **83**, 65 (1999).
 - [7] A. Zanella, M. Chiani, and M. Z. Win, *IEEE Trans. Commun.* **57**, 1050 (2009).
 - [8] J.-P. Bouchaud and M. Potters, *Theory of Financial Risks* (Cambridge University Press, Cambridge, 2001).
 - [9] C. E. Porter, *Statistical Theory of Spectra: Fluctuations* (Academic, New York, 1965).
 - [10] M. L. Mehta, *Random Matrices*, 3rd ed. (Elsevier, Amsterdam, 2004).
 - [11] F. Haake, *Quantum Signatures of Chaos* (Springer, Berlin, 2010).
 - [12] F. J. Dyson, *J. Math. Phys.* **3**, 140 (1962).
 - [13] F. J. Dyson, *J. Math. Phys.* **3**, 157 (1962).
 - [14] F. J. Dyson, *J. Math. Phys.* **3**, 166 (1962).
 - [15] F. J. Dyson, *J. Math. Phys.* **13**, 90 (1972).
 - [16] O. Bohigas, M. J. Giannoni, and C. Schmit, *Phys. Rev. Lett.* **52**, 1 (1984).
 - [17] H. Friedrich and H. Wintgen, *Phys. Rep.* **183**, 37 (1989).
 - [18] B. Eckhardt, *Phys. Rep.* **163**, 205 (1988).
 - [19] O. Bohigas, S. Tomsovic, and D. Ullmo, *Phys. Rep.* **223**, 43 (1993).
 - [20] B. I. Shklovskii, B. Shapiro, B. R. Sears, P. Lambrianides, and H. B. Shore, *Phys. Rev. B* **47**, 11487 (1993).
 - [21] V. E. Kravtsov, I. V. Lerner, B. L. Altshuler, and A. G. Aronov, *Phys. Rev. Lett.* **72**, 888 (1994).
 - [22] A. G. Aronov, V. E. Kravtsov, and I. V. Lerner, *Phys. Rev. Lett.* **74**, 1174 (1995).
 - [23] V. E. Kravtsov and I. V. Lerner, *J. Phys. A: Mat. Gen.* **28**, 3623 (1995).
 - [24] F. Evers and A. D. Mirlin, *Rev. Mod. Phys.* **80**, 1355 (2008).
 - [25] D. Basko, I. Aleiner, and B. Altshuler, *Ann. Phys. (NY)* **321**, 1126 (2006).
 - [26] M. Srednicki, *Phys. Rev. E* **50**, 888 (1994).
 - [27] M. Schreiber, S. S. Hodgman, P. Bordia, H. P. Lüschen, M. H. Fischer, R. Vosk, E. Altman, U. Schneider, and I. Bloch, *Science* **349**, 842 (2015).
 - [28] J. Smith, A. Lee, P. Richerme, B. Neyenhuis, P. W. Hess, P. Hauke, M. Heyl, D. A. Huse, and C. Monroe, *Nat. Phys.* **12**, 907 (2016).
 - [29] J.-y. Choi, S. Hild, J. Zeiher, P. Schauß, A. Rubio-Abadal, T. Yefsah, V. Khemani, D. A. Huse, I. Bloch, and C. Gross, *Science* **352**, 1547 (2016).
 - [30] V. Oganesyan and D. A. Huse, *Phys. Rev. B* **75**, 155111 (2007).
 - [31] M. Serbyn, Z. Papić, and D. A. Abanin, *Phys. Rev. Lett.* **111**, 127201 (2013).
 - [32] V. Ros, M. Mueller, and A. Scardicchio, *Nucl. Phys. B* **891**, 420 (2015).
 - [33] V. Khemani, D. N. Sheng, and D. A. Huse, *Phys. Rev. Lett.* **119**, 075702 (2017).
 - [34] S.-X. Zhang and H. Yao, *Phys. Rev. Lett.* **121**, 206601 (2018).
 - [35] M. Serbyn and J. E. Moore, *Phys. Rev. B* **93**, 041424 (2016).
 - [36] C. L. Bertrand and A. M. García-García, *Phys. Rev. B* **94**, 144201 (2016).
 - [37] N. Chavda, H. N. Deota, and V. K. B. Kota, *Phys. Lett. A* **378**, 3012 (2014).
 - [38] P. Shukla, *New J. Phys.* **18**, 021004 (2016).
 - [39] W. Buijsman, V. Cheianov, and V. Gritsev, *arXiv:1807.05075*.
 - [40] Y. Y. Atas, E. Bogomolny, O. Giraud, and G. Roux, *Phys. Rev. Lett.* **110**, 084101 (2013).
 - [41] A. Pal and D. A. Huse, *Phys. Rev. B* **82**, 174411 (2010).
 - [42] R. Mondaini and M. Rigol, *Phys. Rev. A* **92**, 041601 (2015).
 - [43] D. J. Luitz, N. Laflorencie, and F. Alet, *Phys. Rev. B* **91**, 081103 (2015).
 - [44] D. J. Luitz, N. Laflorencie, and F. Alet, *Phys. Rev. B* **93**, 060201 (2016).

- [45] P. Sierant, D. Delande, and J. Zakrzewski, *Phys. Rev. A* **95**, 021601 (2017).
- [46] P. Sierant, D. Delande, and J. Zakrzewski, *Acta Phys. Pol. A* **132**, 1707 (2017).
- [47] P. Sierant and J. Zakrzewski, *New J. Phys.* **20**, 043032 (2018).
- [48] J. Janarek, D. Delande, and J. Zakrzewski, *Phys. Rev. B* **97**, 155133 (2018).
- [49] D. Wiater and J. Zakrzewski, *Phys. Rev. B* **98**, 094202 (2018).
- [50] R. B. Griffiths, *Phys. Rev. Lett.* **23**, 17 (1969).
- [51] T. Vojta, *J. Low Temp. Phys.* **161**, 299 (2010).
- [52] K. Agarwal, S. Gopalakrishnan, M. Knap, M. Müller, and E. Demler, *Phys. Rev. Lett.* **114**, 160401 (2015).
- [53] K. Agarwal, E. Altman, E. Demler, S. Gopalakrishnan, D. A. Huse, and M. Knap, *Annalen der Physik* **529**, 1600326 (2017).
- [54] K. Kudo and T. Deguchi, *Phys. Rev. B* **97**, 220201 (2018).
- [55] E. Bogomolny, U. Gerland, and C. Schmit, *Eur. Phys. J. B* **19**, 121 (2001).
- [56] V. E. Kravtsov, I. M. Khaymovich, E. Cuevas, and M. Amini, *New J. Phys.* **17**, 122002 (2015).
- [57] I. Dumitriu and A. Edelman, *J. Math. Phys.* **43**, 5830 (2002).
- [58] L. F. Santos and M. Rigol, *Phys. Rev. E* **81**, 036206 (2010).
- [59] J. M. G. Gómez, R. A. Molina, A. Relaño, and J. Retamosa, *Phys. Rev. E* **66**, 036209 (2002).
- [60] M. L. Ndawana and V. E. Kravtsov, *J. Phys. A: Math. Gen.* **36**, 3639 (2003).
- [61] D. Braun and G. Montambaux, *Phys. Rev. B* **52**, 13903 (1995).
- [62] Y. Y. Atas, E. Bogomolny, O. Giraud, P. Vivo, and E. Vivo, *J. Phys. A: Math. Theor.* **46**, 355204 (2013).
- [63] C. Monthus, *J. Stat. Mech.: Theory Exp.* (2016) 073301.
- [64] M. Serbyn, Z. Papić, and D. A. Abanin, *Phys. Rev. B* **96**, 104201 (2017).
- [65] A. D. Mirlin, Y. V. Fyodorov, F.-M. Dittes, J. Quezada, and T. H. Seligman, *Phys. Rev. E* **54**, 3221 (1996).
- [66] A. D. Mirlin, *Phys. Rep.* **326**, 259 (2000).
- [67] I. Varga and D. Braun, *Phys. Rev. B* **61**, R11859(R) (2000).
- [68] S. Welsh and D. E. Logan, *J. Phys.: Condens. Matter* **30**, 405601 (2018).
- [69] D. E. Logan and S. Welsh, *Phys. Rev. B* **99**, 045131 (2019).
- [70] L. Rademaker and M. Ortuño, *Phys. Rev. Lett.* **116**, 010404 (2016).
- [71] C. Monthus, *J. Phys. A: Math. Theor.* **49**, 305002 (2016).
- [72] S. J. Thomson and M. Schiró, *Phys. Rev. B* **97**, 060201 (2018).